REVIEW

Check for updates

Practical considerations in the design and use of porous liquids

Hamidreza Mahdavi, [ID] [a] Stefan J. D. Smith,*[ab] Xavier Mulet*[b] and
Matthew R. Hill [ID] *[ab]

The possibility of creating well-controlled empty space within liquids is conceptually intriguing, and from an application perspective, full of potential. Since the concept of porous liquids (PLs) arose several years ago, research efforts in this field have intensified. This review highlights the design, synthesis, and applicability of PLs through a thorough examination of the current state-of-the-art. Following a detailed examination of the fundamentals of PLs, we examine the different synthetic approaches proposed to date, discuss the nature of PLs, and their pathway from the laboratory to practical application. Finally, possible challenges and opportunities are outlined.

Introduction

In his seminal article in 2007, James introduced the concept of liquids being able to retain porosity permanently.[1] Whilst this remained a concept for several years; eventually, the first porous liquids (PLs) were reported by several research groups.[1–4] Several brief and general reviews have been written by James *et al.*, Bavykina *et al.*, Ahmad *et al.*, Fulvio *et al.*, Jie *et al.*, and Li.[5–11] However, the lack of a comprehensive article investigating the design, synthesis, and applicability of PLs is well felt. Thus, the main aim of this review is to study platform approaches to PL development. Besides, this review aims to frame the drivers for developing this advanced class of material and capture its evolution from initial concept through to implementation at the laboratory scale. We also investigate and discuss a pathway to scale-up PLs, essential for their eventual translation to application. As an alternative to porous solids, PLs show significant potential in a number of important separation processes.

Given the strong link between PL research and their proposed use in separation, we provide a brief overview of the fundamentals of separation processes herein to highlight the potential of PL materials. A separation process is a method that separates distinct compounds within a mixture from each other to yield two or more product mixtures of differing compositions. Such mixtures can exist as either solid, liquid, or gas and often include many components. In general, separation processes are used to enrich one or more of the compounds of a

mixture and in some cases can achieve completely isolate one compound from the rest. Separation is achieved through differences in compounds' physical or chemical properties such as size, shape, mass, density, or chemical affinity.[12,13]

Fundamentally, separation processes are achieved through one of two general modes. The first mode is based on phase-change, whereby the materials are separated *via* the application of heat and/or vacuum and differences in their boiling points. Distillation separation and cryogenic separation are common examples of this separation mode, which are characteristically very energy-intensive.[14] The second mode of separation is where each components' interaction with another material, such as a membrane or sorbent, is used to separate a mixture. In this mode of separation, selectivity is achieved through the difference in permeation or sorption of a component within the separation medium and so careful selection of selective materials can lead to much lower energy consumption among other benefits.[15]

Within the industry, liquid sorbents are implemented in industry, as in liquids being pumped throughout a plant from capture point to regeneration and storage site due to their high adsorption selectivity, good capacity, fast kinetics, and ability to be pumped to different parts of the plant for sorption and release.[2,16,17] While liquid sorbents such as liquid amines often rely on chemical interactions for proper sorption capacity and kinetics, this also results in higher energy requirements for sorbent release and solvent regeneration. Besides, these solvents suffer from some other issues like volatility, and corrosiveness.[18] On the other hand, porous solids adsorb guests to their surface and often exhibit high adsorption capacity, good selectivity, and fast kinetics.[16] A key material characteristic of porous solids is their persistent porosity, and thus high surface area for guest adsorption.[19] Combined with

[a] Department of Chemical Engineering, Monash University, Australia.
 E-mail: Matthew.Hill@monash.edu, stefan.smith@monash.edu
[b] CSIRO, Bag 10, Clayton South, VIC 3169, Australia.
 E-mail: Matthew.Hill@csiro.au, xavier.mulet@csiro.au, stefan.smith@monash.edu

the ability to chemically and/or spatially tailor the surface of pores within the material, porous solids can be tuned for specific separations and are a promising low-energy adsorption technology.[20] However like other solids, they can be difficult to be used in industry and incorporate into a separation process due to the difficulties in maximizing exposed surface areas, separation of particulate material, and complex requirements for handling powders within a process as solid absorbents are more difficult to pump.[17,21] The use of solid sorbents requires the redesign of existing scrubbing facilities, such as the use of fluidized bed reactors using pelletized materials. Pelletization requires additional steps, and it does not guarantee high separation efficiency or easiness of regeneration of solid sorbents or heterogeneous catalysts.[22–24] Operational complexities, unfavourable thermodynamics, and high capital requirements have meant that industry adoption of porous solids has not kept pace with research innovation.

Nevertheless, researchers have sought to develop separation technologies that combine the advantages he porous solids and liquid sorbents is an appealing concept.[25] Porous liquids have emerged as a combination of the properties of fluids such as fluidity and fast mass transfer, which can enable use in continuous cyclic separation processes, and the beneficial aspects of porous solids, such as permanent porosity and molecular sieving and low regeneration temperatures, which can enable the size-selective or shape-selective dissolution of solutes.[26–28]

No matter how counter-intuitive liquids with permanent porosities are, there have been several significant developments in recent years that have brought PLs closer than ever to industrial application. Many significant aspects of PLs have been described so far, including porosity, good adsorption capacity and selectivity, fast kinetics, fluidity, and the demonstration of improved process efficiencies. PLs can be incorporated into current chemical processes like gas sweetening, sprayed, printed, or even formed into films, incorporated into polymers, and show advantages over porous solids. Porous liquids can provide more efficient separation technologies given the possibility to design materials with negligible vapor pressure, low regeneration costs.[5,24] The unusual combination of physicochemical properties displayed by PLs have significant potential for applications across a wide range of fields including gas adsorption and storage, homogeneous catalysis, membrane separation, as well as for pharmaceutical applications.[6,17,25]

Extrinsic and intrinsic porosity

All liquids possess porosity. Molecules in liquids are not rigid and well packed; they are continually tumbling over each other arbitrarily. This leads to the presence of small transient pores that consistently appear and disappear between the molecules in liquids, which is called extrinsic porosity. These pores are short-lived and typically very small, about 1 Å in diameter, and have irregular shapes.[29] This type of porosity is well recognised and considered the significant reason for basic phenomena (dissolution and diffusion) or, in other words, bulk properties of liquids. In essence, the required energy to
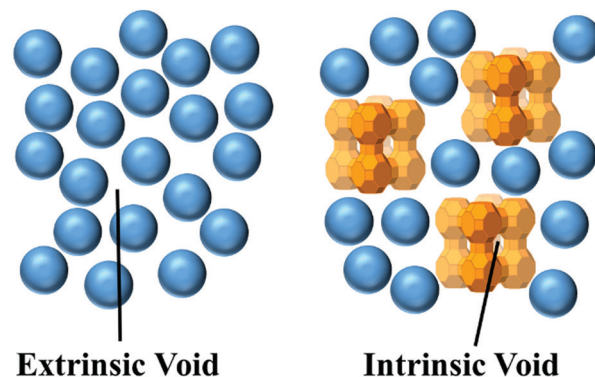

Fig. 1 Schematic images of the critical differences between PLs with intrinsic porosity compared to ordinary liquids with extrinsic porosity (solvent molecules are shown as blue spheres).

separate molecules in liquids from each other and create a pore for the solute is considered the original energy penalty to dissolve a solute in a liquid. The solute's ability to move into neighbouring pores is regarded as the main parameter to control and limit the diffusion rate of a solute throughout a liquid.[30] The disorder present in fluids means that there is no control in the generation of pores between disordered molecules.[5]

In contrast, PLs exhibit both extrinsic and intrinsic porosity, as presented in Fig. 1. Intrinsic porosity relates to the well-defined empty space within the porous molecules (porogen) present in the liquid. Under the right conditions, this porosity is permanent, molecular-sized, and well distributed within the liquid. Through the movement of the porogen, these defined pores also move freely within the fluid.[5] Clearly, it is crucial to prevent the penetration of the solvent or other undesired molecules within the porogen so that the intrinsic pores can be used to adsorb target compounds.[31] Hence, the presence of intrinsic voids within porogens that exclude the solvent and do not self-penetrate result in a true liquid with permanent porosity.[31]

A brief history of porous liquids

General chronological history

The general chronological history of key PL discoveries including the porous solids responsible for the emergence of PLs is illustrated in Fig. 2. From 1944 through to 1988, organic molecules such as crown ethers and calixarenes were the very first examples of neat liquids containing porosity.[32,33] In 1992, novel types of organic cage-like molecules with more complicated shapes like *tert*-butyl calix[4]arenes were developed.[34] However, their shapes and high flexibilities meant that their intrinsic pores could collapse or be readily lost by intermolecular self-filling.[32–34] Furthermore, as presented in 1992, cucurbiturils were considered the very first empty organic hosts in fluids through their dissolution in sterically hindered solvents.[35] In 1994, Cram introduced one of the other early examples of empty organic hosts dissolved in sterically
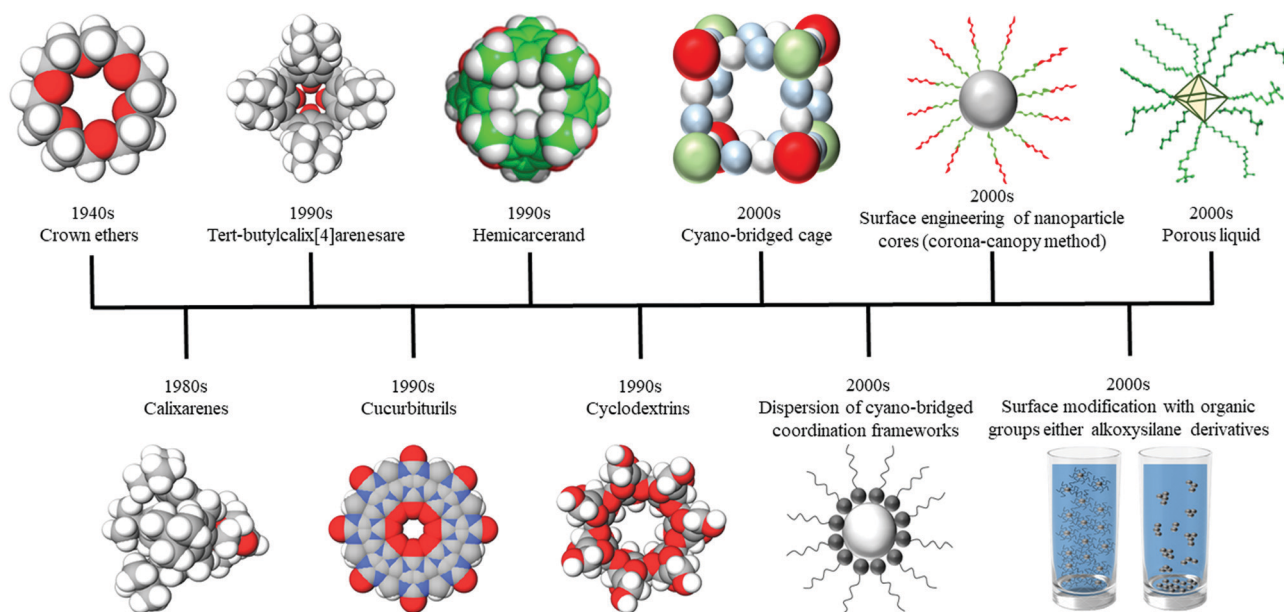
Fig. 2 General chronological history of key PL discoveries.

hindered solvents concept using hemicarcerands. Although the empty structures should not collapse based on the Space-filling model, retaining voids in the liquid solvent was not determined directly.[36] Subsequently, in 1996, cyclodextrins with more regular tube-like shapes were developed. Cyclodextrins can be considered as early examples of neat liquids containing intrinsic porosity; however, no direct evidence of the presence of permanent porosity in the guest-free state was presented.[37–39]

In 2003, inorganic compounds with intrinsic pores in liquids were presented, such as cyano-bridged cage structures like $[(CpCo(CN)_3)_4(Cp^*Ru)_4](Co_4Ru_4)$, which created empty voids when dissolved in sterically or even non-sterically hindered solvents.[40] In 2004 the dispersion of cyano-bridged coordination frameworks also has been investigated.[41] At this time, this field faced significant challenges with few convincing examples of effective demonstrated PLs reported in the literature.

Since then, other approaches to create intrinsic pores have been developed. In 2005, a methodology was established to surface engineer nanoparticles to form a corona-canopy species. This technique lowered the melting point of the overall compound by attaching oligomers or polymers with low melting points as a canopy around the nanoparticle core. The canopy was either ionically grafted to the nanoparticle surface or covalently, and behaved like a fluid medium leading to liquid-like behaviour. In this way, hybrid nanoscale liquids could flow in the absence of any solvent.[42–44] Moreover, in 2006, surface modification with organic groups such as alkoxysilane derivatives or hydrophilic closure molecules, was introduced as a general route for tuning the wettability of dye-loaded zeolite L nanocrystals. This route was shown to form homogeneous and transparent loaded porous solid suspensions in organic solvents by preventing aggregation.[45]

Finally, the concept of PLs was introduced by James in 2007, defining a new class of materials that combined the properties of fluids (such as fluidity and fast mass transfer) with those of porous solids (permanent porosity and molecular sieving).[31] It is important to recognise that many publications may have developed liquids with intrinsic pores before, without knowing the presence of permanent intrinsic pores because assessing it was not straightforward. However, since those examples were not recognised or characterised as such, there is no concrete evidence that PLs had been prepared in those earlier works.[46,47]

Classification and definitions of PLs – advantages and disadvantages

James classified PLs into three types (type I, II, and III) according to their composition and nature, as shown in Fig. 3. type I PLs are neat liquids consisting of molecules that themselves form permanent pores in the liquid state; type II PLs are based on hosts molecules with permanent intrinsic pores dissolved in a liquid solvent that is excluded from the pores; and type III PLs, which contain a porous framework nanoparticle homogeneously dispersed in a liquid solvent in
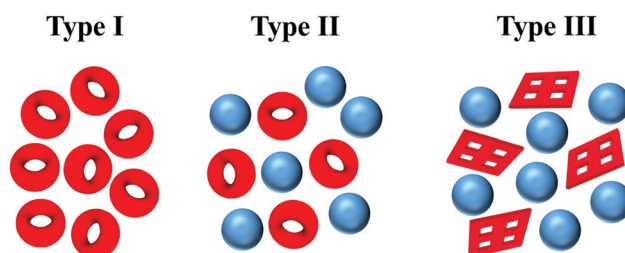
Fig. 3 Structure of the three different classes of PLs.

which the solvent molecules are sterically hindered from entering the pores.[2,31,48,49]

The main advantage of type I PLs is that it is that the concentration of pores is not limited by the low solubility of porogens, or their tendency to settle out of solution. However, the typical synthetic approach to type I PLs is multi-step and complex,[1,3] and the resulting material is often highly viscous. By comparison, the structural and chemical variety and tuneability of type II and III PLs can be more readily modified through changes to either the porogen or solvent molecules present.[26] In types II and III, the amount of open porosity is directly proportional to the concentration of porogens. Thus, given a limited range of sterically hindered solvents, porogens must have extremely high compatibility with the solvent.[5,48,50] Low solubility of porogens is a core disadvantage of type II PL; however, this issue may be addressed through multi-step surface modification.[5] In type III PLs, a core challenge is the tendency of framework porogens to sediment or flocculate, which also yields the need for potential modification of the framework surface.[5,48,50]

Of the three PL moieties described above, type III is likely to be the closest to implementation in current industrial applications. Type III PLs have a relatively facile porogen synthesis route and a wide range of both solvent and porogens that may be accessible. The fundamental challenge of dispersion instability must be overcome to yield a stable dispersion with open porosity with enough guest solubility for specific applications.[5]

Key research developments

Since the inception of the PL, multiple research groups are beginning to translate this concept into reality. Since 2012, the interest in PL research has exploded with a growing number of papers published describing the properties for all three types of PLs.[6] Below we summarise the key papers that have advanced the development of novel PLs.

In 2012, Giri et al. studied the alkylation of organic cages with small internal pores as one of the first methods to realise the fluidity and permanent porosity in a single system. An organic cage was synthesised based on the co-condensation of four 1,3,5-benzenetricarboxaldehyde molecules and six 1,2-ethylene diamine molecules. Normally, these cages do not melt before reaching their decomposition temperature (approximately 573 K), so the diamine groups were alkylated with 12 n-pentyl (n-C$_5$), n-hexyl (n-C$_6$), iso-hexyl (iso-C$_6$), or n-octyl (n-C$_8$) to lower the cage's melting point. However, these alkyl chains can penetrate and fill the cage's cavities. A careful chain length adjustment strategy was thus considered to prevent this chain penetration into the cavities.[1]

In early 2014, Melaugh et al. published the first examples of type I PLs. They added short pentyl chains outside an organic cage molecule to reduce the melting point and retain the porosity. As a result, the melting point from above 573 K was reduced to as low as 313 K. However, the melting point was still too high for the resulting PL to be useful.[4] That same year, Liu et al. dispersed ZIF-8 nanoparticles in glycol and glycol-2-methylimidazole as bulky solvents to create type III PLs. These slurries presented promising adsorption and higher

CO_2/N_2 selectivity in comparison to the pure solvents. The resulting PL also exhibited a lower adsorption enthalpy (-29 kJ mol^{-1}) than aqueous amines (around -100 kJ mol^{-1}) and ionic liquids (mostly above -50 kJ mol^{-1}).[51]

In 2015, Giri et al. published the first two examples of type II PLs; the first studies in which type II PLs were identified and characterized as such. They dissolved porous organic cages in a solvent but found that the loading of organic cage molecules was severely limited by solubility (formed from saturated solutions resulting in precipitation out at elevated concentrations). To address this, crown ether groups were added to the external surface of the organic cage molecules' to increase their compatibility with the bulky crown ethers and chlorinated solvents. The resultant suspension was a liquid at room temperature. The presence of empty pores and cages' ability to uptake gases was confirmed using spectroscopic measurements and molecular modelling, though the gas uptake was found to be lower than most zeolites and MOFs.[3] In 2015, Zhang et al. developed a new type I PL. The concept was the same; however, the liquid comprised empty colloidal spheres at room temperature. They used hollow silica spheres with microporous shells as porogens. Then porogens were rendered into liquid form by functionalizing the external surface using the ionic interactions of polyethylene glycol chains. This methodology could potentially be used to design a range of different PLs. This type I PL can possess considerably more pores per unit volume of the solution compared to other types II and III PLs. Since hollow spheres have a large amount of porosity, similar to that of porous solids, and their microporous shells prevent self-filling after liquefying. Although gas adsorption was not studied, the gas permeability properties were investigated.[2]

The use of ionic liquids as solvents has also been met with some success. Shan et al. used mixtures of the solid porogens ZIF-8, ZSM-5, and Silicalite-1 suspended in a [DBU-PEG][NTf$_2$] ionic liquid solvent to obtain a type III PL. A PL with a high level of stability and homogeneity is dependent on chemical bonding at the interface between nanoparticles and solvent. For instance, the electron-rich species atoms of solvent can interact with the adjutant positive metal ions on the porogens' surface.[48] In 2019, Zhao et al. developed a new PL fundamentally based on the compatibility principle of similar structures and steric interactions between UiO-66 nanoparticles and the [M2070][IPA] ionic liquid. In this work, polyether amine (D2000) was used as a modification agent on the surface of the MOF to take advantage of the structural similarity between the D2000 and M2070 cations. The carboxyl groups of UiO-66 nanoparticles were modified with terminal amine groups of D2000. Subsequently, the modified UiO-66 nanoparticles were dispersed into the [M2070][IPA], which led to a homogeneous and stable PL at room temperature with high CO_2 uptake.[52] Recently, Cahir et al. further advanced the III PL field by exploring a range of solvent and porogen combinations and identifying which ones lead to permanent porosity. The porogens were selected from a series of MOFs, zeolites, and porous organic polymers; while the solvents used included several oil-based solvents suitable for gas separations and biocompatible applications.[50]

Platform approach to porous liquid development

Since 2007, PL synthesis has been mainly based on the 'hard-soft' concept in that pores are considered as the 'hard' section and the chemistry associated with imbuing fluidity is the 'soft' section. These synthetic approaches are summarised below.

Room temperature ionic liquids – disorder and repulsion

The liquid character of ionic liquids at low temperatures compared to high-temperature molten salts arises from Coulomb (long-range) and dispersion (short-range) interactions between the organic-based cations and anions. Typically, the basis for forming a molten salt is the need to input significant energy to overcome the strong, attractive forces between oppositely charged species. On the other hand, ionic liquids can exist in the liquid form at much lower temperatures due to the charge delocalisation of the anion and/or cation, and the low symmetry of ions. Therefore, they require significantly less energy to form and maintain (Fig. 4).[53,54] The charge delocalisation on the anion and shielding of the positive charge on the cation lead to decreasing Coulomb interactions between ions, and facilitates the formation of a low melting point ionic liquid.[55,56] The close-packing of a typical salt lattice is another identified feature that resulted in strong interactions. The significantly lower symmetry of ionic liquids can disrupt or diminish the crystallisation and causes a low melting point. Ions with low symmetry incorporating such as cations with varied lengths of alkyl chains produce more mobility and lower melting points than symmetric cations.[57] Although their criteria are nearly general and can be considered for lots of different species, there are some cases where specific interactions between particular ions provide an exception to these criteria.[58–60]

Fluidising particles

The broad concepts that have driven the development of RTIL can be applied to the development of PLs.[61] In essence, to ensure the system's fluidity, the weak intermolecular forces that pack porogens together should be minimised. However, there is a clear trade-off between fluidity and porosity to overcome.[4] A successfully implemented methodology that enables a single porogen moiety to be fluidised, i.e. type I, is

surface engineering of porogens cores with corona-canopy species to prevent pore occlusion.[1,42,62] This surface engineering results in poor crystal packing and, therefore, a lower melting point.[2,43] However, the downside to using a corona layer on the surface of the porogen is that the canopy may cause more intermolecular self-filling. Unfortunately, self-penetrability of the canopy is driven by the same features introduced to support fluidity such as the molecule's length, flexibility, branching, and the bulk of the chain terminal group.[1,4] Generally, this method is highly flexible and compatible, enabling broad tunability to develop new PLs with desired functionality.[63]

Suspensions in sterically hindered solvents

Another approach that can be used for PLs synthesising is to suspend or dissolve porogens in a solvent, sterically hindered from entering the pores. Thus, intrinsic porosity is retained by preventing solvent penetration into the pores. However, solubility or dispersion stability, driven by increasing the interaction between the porogen and solvent, is the key parameter. Generally, porous materials' solubility or dispersion in solvents are limited. Thus, irrespective of whether the pore is empty, it is essential to consider how solvent chemistry will impact porogens' concentration and stability in solution.[64]

The chain length of porogens can be extended, increasing solubility along with porosity and lower viscosity.[39] It is possible to use this method when porous solids like POCs, MOPs, and COFs are used as porogens.[31] However, one of the main challenges in this method is chain propensity to penetrate the pores, which are functions of the chain length, branching, flexibility, and the bulk of the chain terminal group.[1,4]

Several essential parameters need to be considered to develop a stable dispersion in which porogens remain suspended in a solvent and combine both porosity and fluidity.[31] The key parameters include porogen particle size, solvent-porogen interaction, solvent viscosity, and density. The optimal combination of these parameters requires: (i) decreasing the porogen particle size by rapid crystallisation from solution or ball milling, (ii) increasing the affinity between the porogens and solvent by chemical modification to the surface of porogens or changing solvent, (iii) increasing the solvent viscosity (delay the dispersion sedimentation/flocculation), and (iv) increasing the solvent density (more compatibility with the relatively high-density porogens).[50]

Types of porous liquids

The platform approaches have been used to synthesise different types of PLs. These synthetic approaches for each type of PLs are summarised below.

Type I

Despite all the challenges in designing and preparing PLs, recent reports point to the feasibility of type I PL. Table 1 summarizes the current state-of-the-art PLs, including their composition and properties. In type I PLs, the porogens are
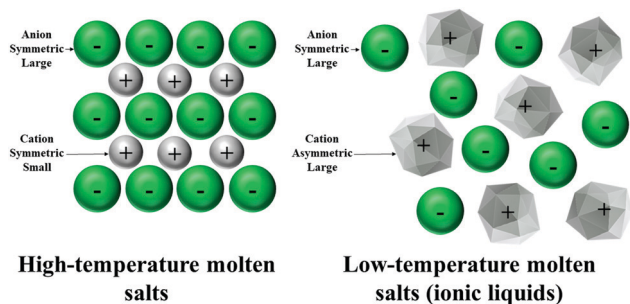

Fig. 4 Schematic images of the differences between the ionic structures of high-temperature molten salts and low-temperature molten salts (ionic liquids).

Table 1 A summary of the current state-of-the-art type I PLs, including their composition and properties

Composition	Pore size (Å)	Specific surface area (m² g⁻¹)	Pore volume (cm³ g⁻¹)	Melting point (K)	Viscosity (mPa s)	Sorption capacity at 1 Bar	Ref.
Tetrahedral organic imine cage functionalised with twelve *n*-pentyl (*n*-C5) chains	5	289	30% unoccupied	423	Extremely high viscous	Five to ten-fold sorption increase than solvent (testing conditions: CH_4, 350 K, 0.1–2 bar)	1 and 4
Porogen: hollow silica nanospheres Corona: *N,N*-didecyl-*N*-methyl-*N*-(3-trimethoxysilylpropyl)ammonium chloride Canopy: poly(ethylene glycol) 4-nonylphenyl 3-sulfopropyl ether Potassium salt	140	—	—	Below 289	6800 (313 K)	—	2
Tetrahedral coordination cage by incorporating 12 poly(ethylene glycol)–imidazolium chains	6.29 ± 0.08	—	—	Below 289	Viscous	—	65
Dicyclohexano-18-crown-6 (18-crown-6/potassium ion complexes as the cationic parts) with an anionic porous organic cage (as the anionic parts)	4.661	—	—	243	Viscous	0.429 mmol g⁻¹ (testing conditions: CO_2, 298 K, 10 bar)	66
Porogen: hollow carbon nanospheres Corona: polymerized ionic liquids Poly(1-vinylimidazole) 3-butyronitrile Canopy: poly(ethylene glycol) 4-nonylphenyl 3-sulfopropyl ether Potassium salt	∼18	314	—	285	—	0.568 mmol g⁻¹ (testing conditions: CO_2, 298 K, 10 bar)	67
Porogen: encapsulated Au, Pt and Pd nanoparticles hollow silica spheres Corona: *N,N*-didecyl-*N*-methyl-*N*-(3-triethoxysilylpropyl)ammonium chloride Canopy: poly(ethylene glycol) 4-nonylphenyl 3-sulfopropyl ether potassium salt	110	163	—	—	Highly viscous	—	68 and 85
Porogen: UiO-66 Crona: *N,N*-didecyl-*N*-methyl-*N*-(3-trimethoxysilylpropyl)ammonium chloride Canopy: poly(ethylene glycol) 4-nonylphenyl 3-sulfopropyl ether Potassium salt	8–11	—	—	303	Highly viscous	0.636 mmol g⁻¹ (testing conditions: CO_2, 298 K, 10 bar)	69
Porogen: hollow silica nanospheres of different sizes Corona: 3-(trihydroxysilyl)-1-propanesulfonic acid Canopy: polyether amine M2070	90	—	—	275.08	660	1.5 mmol g⁻¹ (CP-SIT-M2070)	
	140			273.16	470	2.0 mmol g⁻¹ (F108-SIT-M2070)	
	320			273.77	250	2.2 mmol g⁻¹ (F127-SIT-M2070)	70
					(289 K)	(Testing conditions: CO_2, 298 K, 25 bar)	
Porogen: UiO-66	7	—	—	266.9	4 585 000 (298 K)	1.95 mmol g⁻¹ (UiO-66-liquid-M1000)	

Table 1 (continued)

Composition	Pore size (Å)	Specific surface area ($m^2 g^{-1}$)	Pore volume ($cm^3 g^{-1}$)	Melting point (K)	Viscosity (mPa s)	Sorption capacity at 1 Bar	Ref.
Corona: 3-(trihydroxysilyl)-1-propanesulfonic acid Canopy: polyether amines (M1000, Eth, M2070)					700 000 (353 K)	3.53 mmol g^{-1} (UiO-66-liquid-Eth) 2.68 mmol g^{-1} (UiO-66-liquid-M2070) (Testing conditions: CO_2, 298K, 10 bar)	71
Porogen: hollow carbon sphere with different particle sizes (100, 250, and 450 nm)	—	—	—	283.3	11 2017 (450-P[VHIm]Br-PEGs)	1.05 mmol g^{-1} (CO_2)	
Corona: polymerized ionic liquids such as poly 1-(4-vinylphenyl)methyl-3-butylimidazole chloride salt (P[VBBI]Cl), and poly-1-vinyl-3-heptylimidazole bromide (P[VHIm]Br)				277	75 708 (250-P[VBBI]Cl-PEGs)	0.0901 mmol g^{-1} (N_2)	
Canopy: poly(ethylene glycol) 4-nonylphenyl 3-sulfopropyl ether Potassium salt					57 425 (250-P[VHIm]Br-PEGs) (298 K)	(450-P[VHIm]Br-PEGs) 1.03 mmol g^{-1} (CO_2) 0.0736 mmol g^{-1} (N_2) (450-P[VBBI]Cl-PEGs) (Testing conditions: 298 K, 10 bar)	72
Porogen: silicalite-1 zeolite Corona: N,N-didecyl-N-methyl-N-(3-trimethoxysilylpropyl)ammonium chloride Canopy: poly(ethylene glycol) 4-nonylphenyl 3-sulfopropyl ether Potassium salt	6.1	—	—	Below 289	—	0.474 wt% (testing conditions: CO_2, 1 bar)	79
Porogen: UiO-66 Corona: imidazolium-functionalized organic linker Canopy: poly(ethylene glycol) 4-nonylphenyl 3-sulfopropyl ether Potassium salt	8–11	—	—	301	—	5.93 mmol g^{-1} (Testing conditions: CO_2, 298 K, 9 bar)	80
Porogen: hollow-core and silica-shell nanorods with different aspect ratios	16.1	12	0.017	293	Low viscous	0.758 mmol g^{-1} (PS-OS@SiNR: aspect ratio 2.5)	
Corona: dimethyloctadecyl[3-(trimethoxysilyl)propyl]ammonium chloride	17.4	27	0.088			1.115 mmol g^{-1} (PS-OS@SiNR: aspect ratio 8)	
Canopy: poly(ethylene glycol) 4-nonylphenyl 3-sulfopropyl ether potassium salt	16.1	5	0.155			0.803 mmol g^{-1} (PS-OS@SiNR: aspect ratio 11) (Testing conditions: CO_2, 273 K, 0.03 P/P_0)	81
Hollow silica nanorods-polymer surfactant	150	8.5	≈3% v/v of silica nanorods and ≈16% v/v of polymer surfactant	293	9700 (289 K)	0.223 mmol g^{-1}	
Corona: dimethyloctadecyl [3-(trimethoxysilyl) propyl] ammonium chloride Canopy: poly(ethylene glycol) 4-nonylphenyl 3-sulfopropyl ether potassium salt (Permanent voids/pore volume)						(Testing conditions: CO_2, 273 K, 0.03 P/Po)	82

Table 1 (continued)

Composition	Pore size (Å)	Specific surface area (m^2 g^{-1})	Pore volume (cm^3 g^{-1})	Melting point (K)	Viscosity (mPa s)	Sorption capacity at 1 Bar	Ref.
Covalently linking of UiO-66-OH with oligomer species (polyether amine (M1000, M2070, and T5000) reacted with the organosilane)	—	—	—	268 (UiO-66-OH-OS-M2070)	14 600 (UiO-66-OH-OS-M2070)	0.276 mmol g^{-1} UiO-66-OH-OS-M2070 0.254 mmol g^{-1} UiO-66-OH-OS-M1000 (Testing conditions: CO_2, 298 K, 10 bar)	83
Covalently linking of amino-functionalized ZIFs with the diglycidyl ether-terminated of PDMS with different molecular weights (1000, 4000, and 14 000 g mol^{-1})	6150 ZIF-8@BPEI-PDMS(1000 g mol^{-1}) 7120 ZIF-8-g-BPEI-PDMS(1000 g mol^{-1})	—	—	196 ZIF-8@BPEI-PDMS(1000 g mol^{-1}) ZIF-8-g-BPEI-PDMS(1000) (298 K)	49 ZIF-8@BPEI-PDMS(1000) 59	0.0581 mmol g^{-1} (ZIF-8@BPEI-PDMS(1000)) 0.0475 mmol g^{-1} (ZIF-8-g-BPEI-PDMS(1000)) (Testing conditions: CO_2, 298 K, 1 bar)	84

required to have a low melting point to be a neat PL at acceptable temperatures, which remains a considerable technical difficulty.[44] Typically, the porogens have a high molecular weight due to bulky cages with long chains, as they have to have guest cavities of significant size. This normally results in high melting points.[5] Furthermore, constituent molecules of a neat PL need rigid internal pores that cannot collapse with shapes incapable of intermolecular self-filling.[31] There are several approaches to induce fluidity and lower the melting point of relatively rigid molecular components.

The alkylation of organic cages with molecule-sized pores introduces disorder into the system and permits the decrease of the system's melting point (Fig. 5). This process aims to ensure that the external surface is decorated with alkyl group chains. However, one of the main challenges of this approach is chains may penetrate the cavities both from an intra- and intermolecular perspective.[1] Increasing the steric bulk of the alkyl groups through well-recognised approaches such as the use of branched chains will cause a reduction in this occurrence. However, alkylation with branched chains leads to a higher melting point than linear chains.[4] In essence, although adding chains leads to lower melting points and rendering to liquid form, the length and branch of the alkyl chains may negatively impact the porosity and fluidity of PLs due to penetration into cavities and higher viscosity.[1] Thus, it is essential to carefully consider alkyl chain composition to limit the degree of cavity occlusion as investigated by Melaugh et al.[4]

Another way to increase the accessibility of the pore is to increase the Coulombic repulsion between chains and the ionic liquid's porous, tetrahedral coordination cages. This requires the presence of charge on the surface of the cages. Therefore, the cages should be charged, and chains can be made of two parts. One part can lead to liquid-like behaviour of the cage in the neat state, and the charged moieties that are the same with the cage at the end of the chains prevent chains' penetration into the charged cage pores. One of the main benefits of porous ionic liquids is their negligible vapour pressure induced by their large molecular size. This renders the use of vacuum swing adsorption possible to regenerate their functionality following exposure to a gas moiety.[65] Another interesting approach to make PLs derived from porous solids is the supramolecular complexation strategy. In essence, simple mixing of the anionic porous cage as the anionic parts with cationic counter ion solvent leads to forming a porous ionic liquid.[66] Transforming surface-modified hollow nanospheres or MOFs powder into PLs via an electrical balance strategy (or electrostatic grafting of polymers) is another methodology for preparing type I PLs. The external functionalisation is achieved using corona and canopy species. If the nanospheres' external surface has a charge as grafting sites such as silica, zeolite, or UiO-66, negatively charged organosilane moieties could form a complex with the surface and it can be balanced with positively charged poly (ethylene glycol)-tailed sulfonate salt or polyether amines using an ion-exchange approach.[2,67–72] The higher grafting
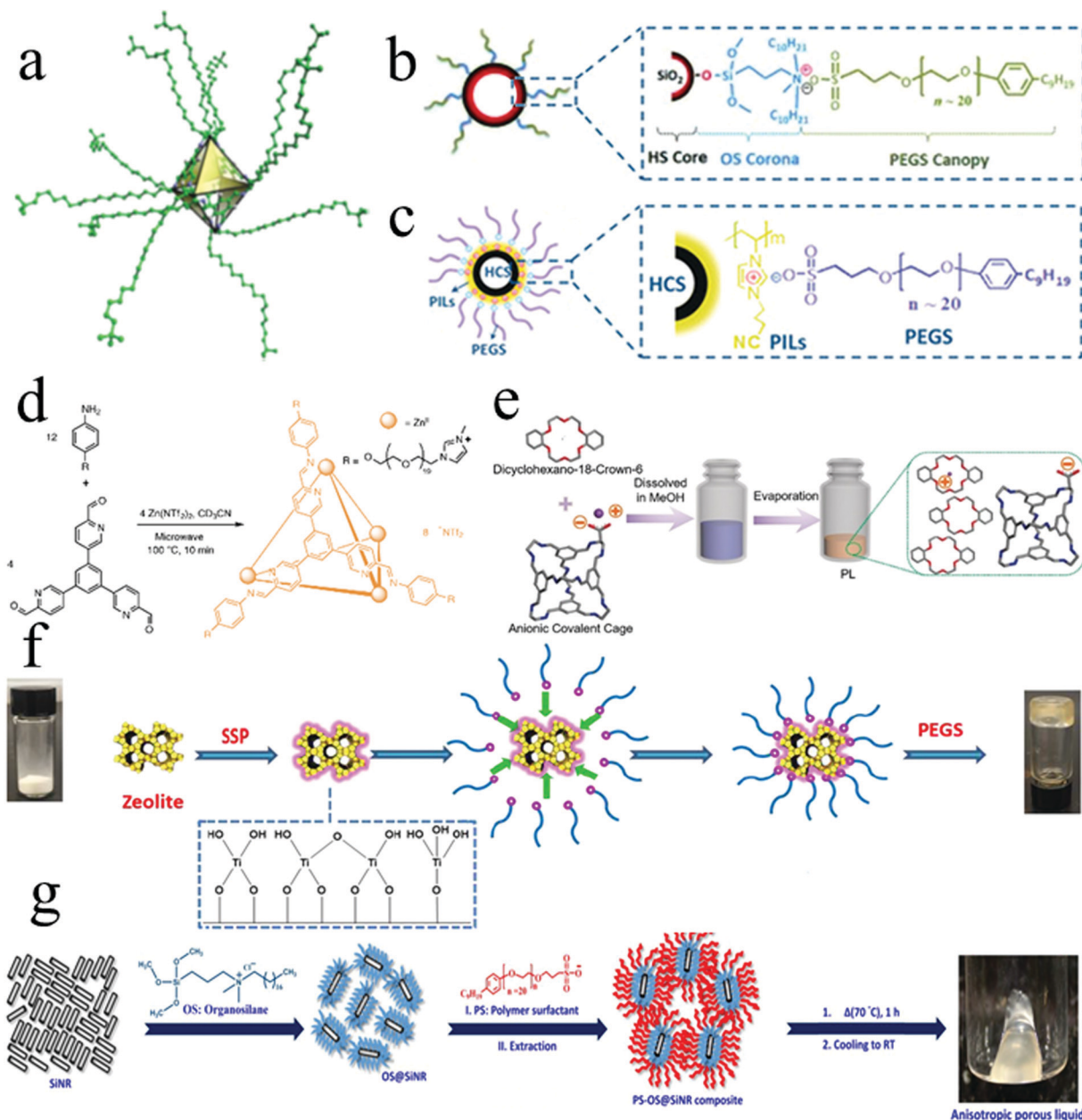
Fig. 5 The schematic preparation process of type I PLs by (a) alkylation of organic cages (reproduced with permission,[4] Copyright 2014, RSC Pub); (b) electrostatic grafting of polymers on the surface of the hollow silica nanospheres (reproduced with permission,[2] Copyright 2015, Wiley-VCH); (c) electrostatic grafting of polymers on the surface of the hollow carbon nanospheres (reproduced with permission,[67] Copyright 2017, Wiley-VCH); (d) electrostatic grafting of polymers on the surface of ionic-liquid, porous, tetrahedral coordination cage (reproduced with permission,[65] Copyright 2020, Springer Nature); (e) anionic porous organic cage and dicyclohexano-18-crown-6 using a supramolecular complexation strategy (reproduced with permission,[66] Copyright 2020, Wiley-VCH); (f) electrostatic grafting of polymers on the surface of the Silicalite-1 Zeolite (reproduced,[79] Open access); and (g) electrostatic grafting of polymers on the surface of the anisotropic (directionally dependent) hollow-core and silica-shell nanorods (reproduced with permission,[81] Copyright 2019, RSC Pub).

density leads to more repulsive forces and consequently better stability. In contrast, due to more polymer chains tangled with each other, the PLs' viscosity increased while sorption decreased because of more pore blockage.[73] Besides, reducing the pore size to an acceptable range was desirable for stability and fluidity, while gas sorption decreased because pore sizes were easily blocked by canopy.[74] Moreover, the linear and long

canopy structures caused lower viscosity and better fluidity. This is due to the fact that the steric hindrance effect in these structures precipitates smaller relative entanglement depth and better dispersion. They also help keep the intrinsic pores empty more appropriately.[75] More importantly, nanospheres synthesis can be modified by different factors such as calcination temperature, surfactant concentration as well as micelle swelling

agent concentration to be able to control the size of internal cavities and nanospheres along with the microporosity of the silica shell. Thus, the cavity accessibility can be adjusted.[76]

However, the lack of sufficient grafting sites on the surface limits the surface modifications.[77,78] There are different approaches to increase the grafting sites. The organic linkers modification as a pre-modification process or a sol–gel modification on the external surface as a post-modification process may be necessary to ensure future PL stability to maximise the number of sufficient grafting sites on the surface of the porogen.[79,80] The external surface of some porous solids such as MOFs can be formed from imidazolium-functionalized organic linker groups with long carbon chains grafted on the imidazolium groups.[80] Inert external surfaces such as porous hollow carbon nanospheres can adsorb polymerised ionic liquids onto the surface through hydrogen-bond interaction.[67] The adsorbed polymerised ionic liquids or long carbon chains grafted on the imidazolium groups act as a positively charged corona which is balanced with counter-anions. Anion exchange can render the hollow nanospheres into liquid form. The main challenge is that the PLs are highly viscous but flow under gravity. The amount of gas solubility highly depends on the internal cavity sizes. In essence, gas solubility might not be expected to be increased much by the presence of large pores.[2,67–69,79,80] Moreover, anisotropic porous solids such as hollow-core and silica-shell nanorods can be used to decrease the PL's viscosity. This class of porous solids, due to their morphology, possess advantages over their spherical counterparts. For instance, anisotropic porous solids can form a connecting network with a lower percolation threshold volume fraction compared to nanospheres, resulting in easier network formation and gelation. This leads to lower viscosity and plays an essential role in flow-related processes. In addition, the PL's viscosity can be tuned by changing the aspect ratio, packing fraction, and attractive potentials.[81,82]

Recently covalent linkage strategy as a method capable of improving PL fluidity, broadening a liquid range and increasing gas adsorption, and separation performances have been used to form PL. In this method, covalent linkage of the amino end groups of amino-functionalized MOFs was achieved either by impregnation or grafting branched polymer with amine groups with economical industrial raw materials. PLs can be easily tuned by adjusting the porous solid structure, molecular weight, and graft amount of organic outer layers. Therefore, this method leads to lower viscosity and melting point in type I PLs and provides ever-expanding applications, especially in low-pressure gas capture and separation.[83,84]

Type II – vs. type III

In type II and III PLs, the porogens exist in a solvent.[86] Three-dimensional porous solids such as porous organic cages (POCs), metal–organic polyhedra (MOPs), covalent organic frameworks (COFs), porous aromatic frameworks (PAFs), metal–organic frameworks (MOFs), and zeolite can be used as porogens.[31,87] Moreover, POCs[88] and MOPs[89] are two new types of porous solids that have been developed in the last decade.

These porous solids have molecules with a rigid structure and accessible intrinsic cavities. Therefore, they can be considered promising materials in providing tunable void architectures. They have potential in selective gas storage and/or separation, sensing, and catalysis.[90] COFs are another novel type of porous solids with extended crystalline structures.[91] COFs are made entirely from light elements (H, B, C, N, and O) in which building blocks are linked by covalent rather than coordination covalent bonds.[92] COFs can be functionalized into lightweight materials optimized for various applications.[93,94] PAF is a porous solid which also was synthesised by Côté et al. in 2005.[93] PAFs possess very high surface areas, excellent physicochemical stability, and exceptional selectivity for greenhouse gases.[95] MOFs are microporous materials, which consist of interconnected metal-containing nodes and organic linkers. MOFs can form extensive crystalline structures with molecular dimension structures of voids and channels which are accessible through pores.[87] Despite all of the design and preparation challenges in developing PLs, some recent successes have been reported. These demonstrate the proof-of-concept type II and III PLs. The door is now open for new developments. In types II and III PLs, porogen moieties are not required to have a low melting point due to the solvent providing the fluid matrix.[40] The presence of a solvent in types II or III PL means that the porogen system should be rigid, stable, and so unable to collapse when emptied from any guest within its structure. As outlined in the previous section, porogen systems should have restricted access windows (i.e. window size of COF-300, PAF-1, UiO-66, ZIF-8, and ZSM-5 are 7.94 Å, 13.5 Å, 7 Å, 3.4 Å, and 5.4 Å diameter, respectively) to control the entry of guest molecules into the porogen.[31,45] A facile methodology to enable this is to have a small window to use the size/shape exclusion principle.[52] Therefore, the solvent should be rigid sterically excluded from the pores of the porogen.[42,45]

However, the solvent must meet a range of criteria to enable the formation of a PL. For this purpose, the solvent minimum dimensionality should be significantly larger than the porogen's largest windows. Thus, solvent shapes such as linear, branched, spherical, triangular, rectangular, rod, and disk, along with their dimensions (width, height, and depth), are essential aspects to consider.

For instance, a solvent with a linear shape can penetrate porogen pores, while a solvent with a branched shape has significantly hindered diffusion into the pores.[96] The solvent's ease of availability, chemical/thermal stability, biocompatibility, low vapour pressure, low melting point, low specific heat, non-corrosiveness, and low viscosity and density are also important considerations depending on the application.[43,96] A solvent with high chain mobility and weak interaction with gas molecules will lead to high diffusion coefficients, which will enable rapid mass transport of gas molecules.[57] Attention must also be paid to solve viscosity, such that the final PL has low viscosity to facilitate both mass transport and handling. Identifying the appropriate porogen system-solvent combination that meets these multiple criteria is non-trivial and significantly challenging.[42]

The diffusion of guest species limits the PL adsorption through the solvent.[25] The mixture compatibility of porogens and solvent determines if type II or III PL has been formed. Type II PL is porogen dissolved in a sterically hindered solvent. In this PL, a colloidal porogen in the solvent has been formed. Type III PL is porogen dispersed in sterically hindered solvents. In this PL, a porogen slurry in the solvent has been formed.[31] In both cases, the compatibility principle of similar structures and steric interactions can help to increase the solubility or dispersion.[69] Type II PLs and type III PLs can offer many more degrees of freedom from the designer's point of view due to the considerable number of porogens and solvents with various properties.[7]

Table 2 summarises the type II PLs that have been developed. Several strategies have been used to synthesise PLs. A common route to make a type II PL dissolving porogens in a sterically hindered solvent. Several synthetic approaches have been undertaken to overcome the fact that the porogens are usually solubility limited. These approaches are generally based on the compatibility principle of similar structures, and it is possible to increase the compatibility of porogens and solvents. For this purpose, the external surface of porous cages can be functionalised with solvent-compatible groups to enhance compatibility between porogens and solvent. The first approach was employed by Giri et al.,[3] as well as Zhang et al.[97] and later by Greenaway et al.[25]

Solvent selection is also a key path to type II PL development. An example used by Giri et al. is the use of hexachloropropene (PCP) as a bulky solvent as it is unable to penetrate the pores. Based on this approach, the prepared PL flow at room temperature and the solvent penetration into the pores is energetically very unfavourable. However, it suffers from high viscosity, the multi-step synthesis procedure of the cage, the low yield, and limited pore volume due to the high content of functional groups on the surface. Moreover, PCP volatility is also a limiting parameter for practical applications.[3]

To address the mentioned issues, covalent scrambling strategies can be used. This strategy is based on synthesising cages with varying numbers of vertex substituent groups. For instance, two-component scrambled cage mixtures (vertex-disordered) are synthesised through a one-step reaction with varying ratios of structural groups. A vertex-disordered with shorter structural groups disrupts crystal packing and increases disorder. Lower lattice energy can lead to the reduction of the crystallisation propensity, enhancing the cages' solubility in a solvent and getting around external functionalisation. Thus, a mixture of both unsymmetrical and symmetrical cages with randomly scrambled short structural groups over the various cage vertices can be made. The short structural groups are not able to penetrate the cages. Then the scrambled porous cages can dissolve in the solvent and leads to vertex disordered PLs formation with lower viscosity. For instance, as presented in Fig. 6, the scrambled cage mixture was synthesised using in one step the reaction of 1,3,5-triformylbenzene with varying ratios of 1,2-diamino-2-methylpropane and 1,2-diaminocyclohexane. Thus, a combination of both unsymmetrical and symmetrical

cages was randomly scrambled. The diamine groups were not able to penetrate the cages.[3,98]

It can be challenging to predict the composition of the two-component scrambled cage mixtures due to unknown relative reactivities. Thus, three-component scrambled cage mixtures with specific amounts can be used. These cages can obtain more pore concentration up to three times along with higher gas uptake than the best previously reported scrambled cage PL.[99] The gas uptake capacity of vertex disordered PLs correlated with the adsorption heats of the respective scrambled cage. Thus, gas selectivity in these PLs can be governed by the constituent scrambled cages' structure and interactions, which means the properties of porous solids can be translated into PLs. For instance, pore window size reduction leads to switching selectivity from Xe to CH_4. This was a promising approach to tuning gas selectivity by using chemistry in PLs.[100] It was recently found that cages have van der Waals interactions with solvent molecules. However, solvent self-association faced minor disruptions. Furthermore, cages can self-interact, contributing to fluid stabilization.[101]

It is also possible to use a supramolecular complexation strategy to transformed porous solids to type II PL. The simple dissolving of anionic porous cages or metal–organic polyhedra (MOP) with the cationic solvent leads to forming a PL. It is possible to use an excessive amount of solvent or dissolve them under temperature. The interaction between solvent species around porous solids leads to solvent distribution around porous solids.[66,102]

The first examples of type III PLs were prepared by Liu et al. and Lei et al.; MOFs such as ZIF-7 and ZIF-8 were dispersed in bulky solvents like glycol, a mixture of glycol and 2-methylimidazole, a mixture of glycol and water, and ionic liquids like $[P_{6,6,6,14}][NTf_2]$ which leads to the formation of slurries as shown in Fig. 7. Mixing the solvent to decrease the viscosity and increase adsorption was another approach to improve performance.[26,51,103–106] This class of PLs has been extended by using MOFs containing unsaturated metal centres that can induce an effective charge of the metal atom in the direction of the open metal site. It leads to more electrostatic interactions. It can help to increase stability and also adsorption strength.[107] PLs based on aqueous systems were another to improve the system. In this approach, the PL is formed, dispersed in water, and stirred until homogenous. Although using water leads to considerably higher uptake and decreases viscosity, it should not penetrate suspended ZIF-8 pores (Table 3).[108]

In order to get rid of sedimentation issues, it is important to make a stable dispersion. For this purpose, porous solids and solvents should form chemical bonding at the nanoparticle–solvent interface.[48,109] Porous solids solvating in a solvent because of the compatibility produce electron clouds and long-range charge density oscillations that lead to steric repulsion and prevent interpenetration of the porous solids.[109] Besides, the long solvent chains can enter into porous solid channels at the interface and leads to interfacial mechanical bonds. These three phenomena resulted in a homogeneous and

Table 2 A summary of the current state-of-the-art type II PLs, including their composition and properties

Composition		Pore size (Å)	Pore volume (cm^3 g^{-1})	Viscosity (mPa s)	Solubility	Stability	Sorption capacity	Ref.
Porogen	Solvent							
Tetrahedral organic imine cage functionalised with six crown ether substituents	15-crown-5 (15-C-5)		100% of the cages remained empty at all times	20–>140 (Crown cage/ PCP or Crown cage/ 15-crown-5, 298–323 K)	High	—	52 μmol g^{-1} (testing conditions: crown cages/15-crown-5, 8.3% mol mol^{-1} porogen, CH_4, 303 K, 1 bar)	3 and 97
Scrambled cage mixture	Hexachloropropene (HCP)	5		11.7 (Scrambled cage (R)-3^3:13^3/PCP, 295 K, 0.112 mmol g^{-1} PCP)			51 μmol g^{-1} (testing conditions: crown cage/PCP, 8.3% mol mol^{-1} porogen, CH_4, 293 K, 1 bar)	
							234–242 mg ml^{-1} (testing conditions: scrambled cage (R)-3^3:13^3/PCP, 10 wt% porogen, CH_4, 293 K, 1 bar)	
Two-component imine scrambled cage mixtures	15-Crown-5 (15-C-5)	5	0.64% increase	3.73–10.60 (, porogen range of 2.5 −20% w/v, 298 K)	Very high	Stable	55 μmmol g^{-1} (testing conditions: scrambled cage CC3-R/PCP, porogen 20% w/v, CO_2, 298 K, 10 bar)	25
	1,2,4-TrichloroBenzene Perchloroethylene Hexachloropropene Benzyl benzoate [Bmim].[BF_4]							
Anionic porous organic cage	15-Crown-5 (15-C-5)	4.022	—	Viscous	—	—	0.375 mmol g^{-1} (testing conditions: KACC/15-C-5, porogen 0.54 wt%, CO_2, 298 K, 10 bar)	66
Three-component imine scrambled cage mixture (3^3:13^3)	2,4-Dichlorobenzyl chloride (DCBC)	5	0.64% (3^3:13^3/ DCBC)	14.93 ± 0.038 (3^3:13^3/ DCBC)	Extremely high	Stable	14.1 μmol mL^{-1} CH_4 and 47.6 μmol mL^{-1} Xe	99
	Methyl salicylate (MS)		0.66% (3^3:13^3/TBA)	32.46 ± 0.53 (3^3:13^3/TBA)			(3^3:13^3/DCBC)	
	2,4-Dichlorotoluene (DCT)		0.63% (3^3:13^3/MS)	9.84 ± 5.7 10^{-4} (3^3:13^3/ MS)			18.9 μmol mL^{-1} CH_4 and 105.5 μmol mL^{-1} Xe (3^3:13^3/TBA)	
	4-(Tri-fluoromethoxy) benzyl alcohol (TBA)		0.66% (3^3:13^3/DCT)	3.70 ± 0.0031 (3^3:13^3/DCT)				
	2-Hydroxya-cetophenone (HAP)		0.65% (3^3:13^3/HAP)	9.82 ± 0.015 (3^3:13^3/HAP)			20.5 μmol mL^{-1} CH_4 and 77.6 μmol mL^{-1} Xe (3^3:13^3/MS)	
	Perchloropropene (PCP)		PLs – 20% w/v	(Porogen 20% w/v, 298 K)			17.6 μmol mL^{-1} CH_4 and 70.4 μmol mL^{-1} Xe (3^3:13^3/DCT) 25.5 μmol mL^{-1} CH_4 and 101.0 μmol mL^{-1} Xe (3^3:13^3/HAP) 81.7 μmol mL^{-1} CH_4 and 155.0 μmol mL^{-1} Xe (3^3:13^3/PCP) (Testing conditions: porogen 20% w/v, 298 K, 1 bar)	

Materials Horizons

Table 2 (continued)

Composition		Pore size (Å)	Pore volume (cm³ g⁻¹)	Viscosity (mPa s)	Solubility	Stability	Sorption capacity	Ref.
Porogen	Solvent							
The mixture of tetrahedral organic imine cages bearing scrambled CH_3 and $(CH_2)_4$ substituents	Hexachloropropene (HCP)	5	—	4.36 ($CC3^3$:13^3-R/HCP, porogen 4% w/v, 298 K)	High	—	11.6 ± 0.7 μmol g⁻¹ (CH_4)	100
				4.18 (CC15-R/HCP, porogen 5% w/v, 298 K)			10.9 ± 0.8 μmol g⁻¹ (CO_2)	
							16.5 ± 1.0 μmol g⁻¹ (Xe) 2.72 ± 0.38 μmol g⁻¹ (N_2) (Testing conditions: R-$CC3^3$: 13^3-R/HCP, porogen 4% w/v, 298 K, 1 bar) 13.3 ± 1.6 μmol g⁻¹ (CH_4) 7.0 ± 2.0 μmol g⁻¹ (CO_2) 4.25 ± 0.39 μmol g⁻¹ (Xe) 3.87 μmol g⁻¹ (N_2) (Testing conditions: CC15-R/HCP, porogen 5% w/v, 298 K, 1 bar)	
Metal–organic polyhedra (MOP-18)	15-crown-5 (15-C-5)	3.8 (triangular windows)	11% increase	22.5 (porogen 5 wt%, 313 K)	Function of temperature and porogen (PL-up to 30 wt% high solubility at 333 K while low solubility at 298 K. Besides, PL-5 wt% soluble at 313 K)	Function of temperature and porogen (PL-up to 30 wt% quite stable at 333 K while precipitating out within 24 h at 298 K. Besides, PL-5 wt% stable at 313 K)	0.157 mmol g⁻¹ (testing conditions: porogen 5 wt%, CO_2)	102
		6.6 (square windows)						

stable PL.[110] Moreover, to prevent pre-aggregation and lead to a stable solution, it is possible to use wet porous solids, for instance, in methanol instead of the dry porous solid. Indeed surrounded porous solid with methanol is an efficient approach to avoid aggregation before dispersing.[64]

Sometimes simple mixing between compatible porous solid and solvent is enough to form a stable dispersion.[111] However, it is possible to use different approaches to increase the compatibility, and consequently, stability like porogens surface functionalisation, modifying particle sizes, solvent functional groups, solvent density, and viscosity.[27,50] For instance, MOF-based type III PLs have been developed with different strategies. First, the external surface of MOFs has been functionalised to provide better dispersion. Then, an agent with similar structures with positive ions of an ionic liquid as a solvent can modify the external groups of MOF nanoparticles. Then modified MOF nanoparticles were dissolved well into the solvent leading to a homogeneous and stable PL at room temperature.[52]

The other strategy can be polymer coating onto MOF surfaces. The polymer coating can be done through a surface-initiated atom transfer radical polymerisation, situ strategies, or wet impregnation method. Then the modified MOFs were mixed with liquid polymer resulting in an efficient electrostatic repulsion strategy to prepare stable and homogeneous type III PL.[112,113] A novel and easy in situ coupling strategy to prepare type III PL was recently proposed. The aqueous solution of hollow carbon nanospheres was dispersed in an aqueous polymerised ionic liquid solution under stirring. The resulting solution was dried at 323 K under vacuum to get the carbon PL. The key to achieving a PL through this approach relies on the polymerized ionic liquids. The polymerized ionic liquids consist of many ionic liquid units and a large molecular weight backbone like a comb or branched polymeric liquid medium at room temperature. The large backbone prevents ionic liquid units from filling the microporous shell of hollow cavities. The cation–π liquid–particle interaction between polymerized ionic liquids and hollow carbon nanospheres leads to
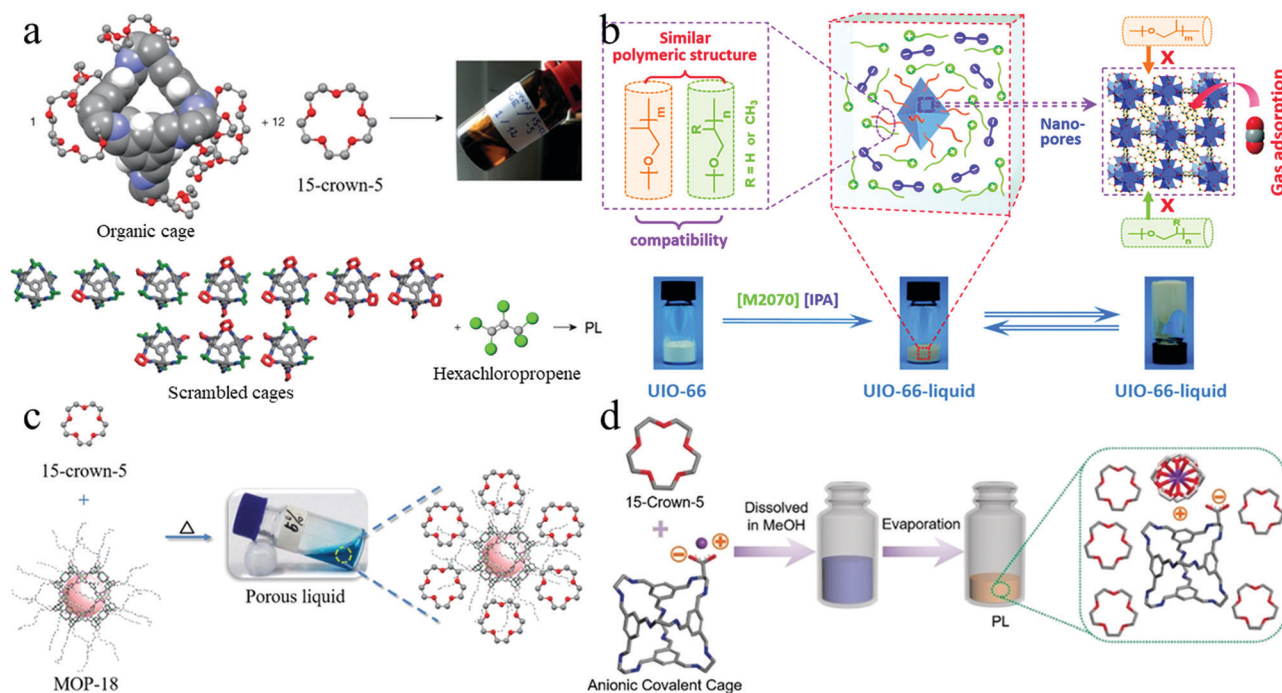
Fig. 6 The schematic preparation process of type II PLs by (a) functionalized tetrahedral porous organic cage dissolving in 15-crown-5 and scrambled cage mixtures dissolving in PCP (reproduced with permission,[3] Copyright 2015, Springer Nature); (b) modified UiO-66 nanoparticles dissolving in [M2070][IPA] (reproduced with permission,[52] Copyright 2019, RSC Pub); (c) MOP-18 dissolving in 15-crown-5 (reproduced with permission,[102] Copyright 2020, Wiley-VCH); and (d) anionic porous organic cage dissolving in 15-crown-5 (reproduced with permission,[66] Copyright 2020, Wiley-VCH).
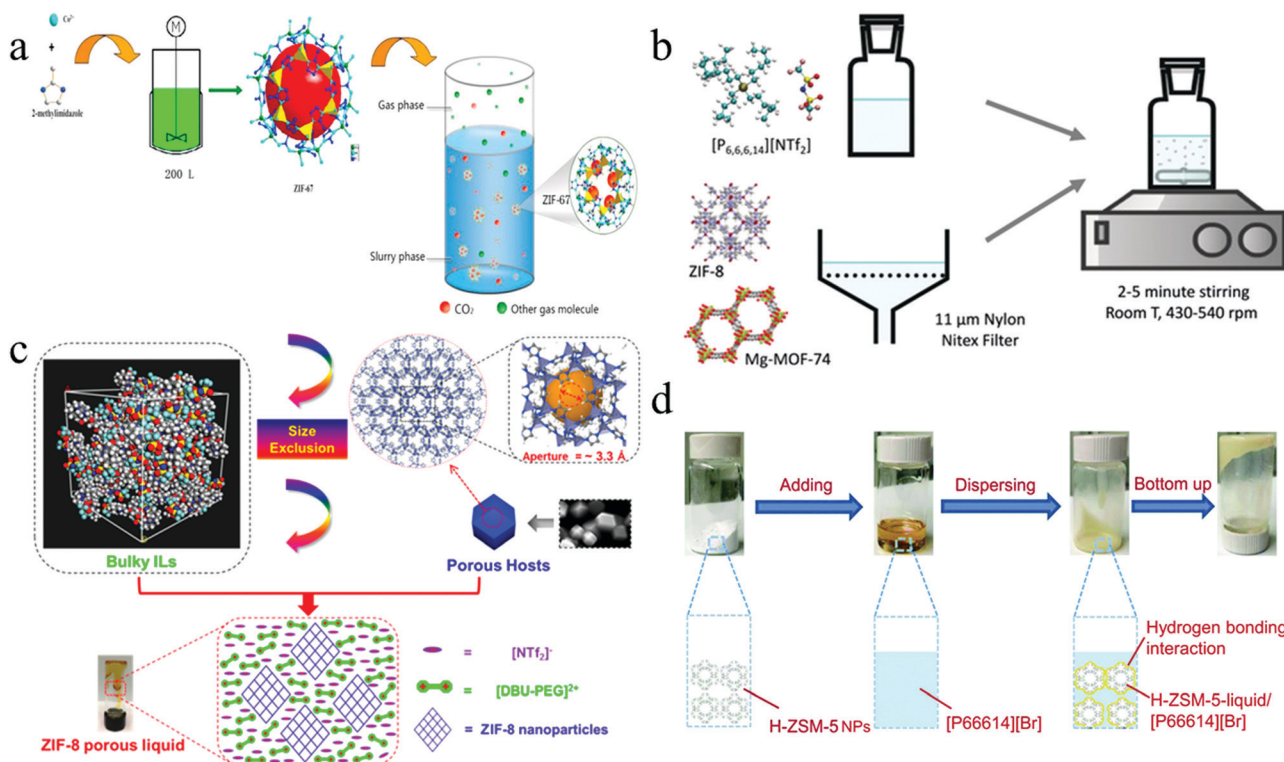

Fig. 7 The schematic preparation process of type III PLs by (a) ZIFs nanoparticles dispersion in glycol-2-methylimidazole (reproduced with permission,[26] Copyright 2018, Wiley-VCH); (b) ZIF-8 and Mg-MOF-74 dispersion in [P6,6,6,14][NTf$_2$] (reproduced with permission,[107] Copyright 2018, Elsevier); (c) ZIF-8, ZSM-5, and Silicalite-1 nanoparticles dispersion in [DBU-PEG][NTf$_2$] (reproduced with permission,[48] Copyright 2018, American Chemical Society); and (d) H-ZSM-5 nanoparticles dispersion in [P66614][Br] as a branched ionic liquid solvent (reproduced with permission,[110] Copyright 2009, RSC Pub).

Table 3 A summary of the current state-of-the-art type III PLs, including their composition and properties

Composition		Pore size (Å)	Specific surface area (m² g⁻¹)	Pore volume (cm³ g⁻¹)	Viscosity (mP s)	Dispersity	Stability	Sorption capacity	Ref.
Porogen	Solvent								
ZIF-8	$[P_{6,6,6,14}][NTf_2]$	3.4	0.663	—	—	Homogeneous	Stable	0.47 mmol g⁻¹ (CO_2) 0.21 mmol g⁻¹ (CH_4) 0.11 mmol g⁻¹ (N_2) (Testing conditions: porogen 5 wt%, 303 K, 5 bar)	26
HKUST-1	Sesame oil	10/14	1695	0.71 (HKUST-1)	—	Homogeneous	Stable	0.67 mmol g⁻¹ (C_2H_6)	27
Zeolite AgA	[BMIM][TFSI] saturated with silver triflate	4.35	—					0.84 mmol g⁻¹ (C_2H_4) (HKUST-1/sesame oil, porogen 12.5 wt%)	
Cu(Qc)₂		3.3	340					0.02 mmol g⁻¹ (C_2H_6)	
ZIF-7		2–5.2	377					0.61 mmol g⁻¹ (C_2H_4) (Zeolite AgA/AgIL, porogen 12.5 wt%) 0.04 mmol g⁻¹ (C_2H_6) 0.84 mmol g⁻¹ (C_2H_4) (Zeolite AgA/AgIL, porogen 25 wt%) 0.28 mmol g⁻¹ (C_2H_6) 0.11 mmol g⁻¹ (C_2H_4) (Cu(Qc)₂/sesame oil, porogen 12.5 wt%) 0.28 mmol g⁻¹ (C_2H_6) 0.11 mmol g⁻¹ (C_2H_4) (ZIF-7/sesame oil, porogen 12.5 wt%) (Testing conditions: 298 K, 0.8 bar)	
ZIF-8	[DBU-PEG][NTf₂]	∼3.3	1297	0.58	Viscous oil (ZIF-8/[DBU-PEG][NTf₂])	Homogeneous (ZIF-8/[DBU-PEG][NTf₂])	Extremely stable (ZIF-8/[DBU-PEG][NTf₂])	1.56 mmol g⁻¹ (ZIF-8/[DBU-PEG][NTf₂], porogen 30 wt%)	48
ZSM-5		5.1	289	0.13				0.46 mmol g⁻¹ (ZSM-5/[DBU-PEG][NTf₂], porogen 5.3 wt%)	
Silicalite-1		5.3	208	0.10				0.38 mmol g⁻¹ (Silicalite-1/[DBU-PEG][NTf₂], porogen 2.1 wt%) (Testing conditions: CO_2, 298 K, 10 bar)	
HKUST-1	Silicone oils	—	—	—	—	Several homogeneous combination	Several stable combination	0.72 mmol g⁻¹	50
ZIF-8	Polyethylene glycols							(PAF-1/Genosorb, porogen 12.5 wt%)	
UiO-66	Naturally occurring triglyceride oils such as olive oil, castor oil, etc							0.36 mmol g⁻¹ (PL-Al(fum)(OH)/PDMS 50 cst, porogen 12.5 wt%)	
UiO-67								0.22 mmol g⁻¹ (ZIF-8/PDMS 50 cst, porogen 12.5 wt%)	
MOF-801								0.22 mmol g⁻¹ (Zeolite 5A/PDMS 50 cst, porogen 12.5 wt%) (Testing conditions: CO_2, 298 K, 5 bar)	
MIL-53(Al) CAU-10 Zeolites CD-MOF-1 PAF-1									

Table 3 (continued)

Composition		Pore size (Å)	Specific surface area (m² g⁻¹)	Pore volume (cm³ g⁻¹)	Viscosity (mP s)	Dispersity	Stability	Sorption capacity	Ref.
Porogen	Solvent								
ZIF-8	Glycol	3.4	—	—	—	Slurry	—	2.82 mol L⁻¹ (CO₂, 11.5 bar)	51
	Glycol-2-methylimidazole							0.06 mol L⁻¹ (CH₄, 6.4 Bar)	
								0.04 mol L⁻¹ (N₂, 6.9 bar) 0.03 mol L⁻¹ (H₂, 6.5 Bar) (Testing conditions: ZIF-8/Glycol, porogen 15.2 wt%, 293.15 K) 7.09 mol kg⁻¹ (CO₂, 41.3 bar) 1.66 mol kg⁻¹ (CH₄, 41.3 bar) 0.57 mol kg⁻¹ (N₂. 42.4 bar) 0.46 mol kg⁻¹ (H₂, 43.2 bar) (Testing conditions: ZIF-8 15 wt%/mIm 34 wt% + glycol 51 wt%, 303.15 K)	
UiO-66 nano-particles modified with polyether amine (D2000)	[M2070][IPA]	5–9	—	—	11.2 Modulus per Pa (Viscous)	Homogeneous	Extremely stable	1.66 mmol g⁻¹ (testing conditions: CO₂, 298 K, 10 bar)	52
ZIF-8	[Bpy][NTf₂]	~3.3	—	—	—	Homogeneous	Extremely Stable	2.51 mg g⁻¹ (CO₂) 0.09 mg g⁻¹ (CH₄) (Testing conditions: ZIF-8/[Bpy][NTf₂], porogen 1.4 wt%, 298 K)	64
ZIF-7	[EMIM, TF₂N]	4.31	20	0.8062				0.0624 mmol g⁻¹ (ZIF-8)/[EMIM, TF₂N], porogen 13.04 wt%, CO₂, 11.24 bar	103
ZIF-8	[OMIM, PF₆]	11.6	1062	0.5926	—	—	—	0.0824 mmol g⁻¹ (ZIF-8/[OMIM, PF6], porogen 13.04 wt%, 17.34 bar) 0.0520 mmol g⁻¹ (ZIF-7/[EMIM, TF₂N], porogen 13.04 wt%, 11.06 bar) 0.0515 mmol g⁻¹ (ZIF-7/[OMIM, PF₆], porogen 13.04 wt%, 10.94 bar) (Testing conditions: CO₂, 298 K)	
ZIF-8	Glycol–water	—	—	—	19 (ZIF-8 20 wt%-Glycol 20 wt% + water 80 wt%, 293.15 K)	Slurry	—	1.14 mol L⁻¹ (ZIF-8/Glycol, porogen 18.3 wt%, C₂H₆, 9.3 bar)	104
								1.07 mol L⁻¹ (ZIF-8/Glycol, porogen 18.3 wt%, C₂H₄, 11.3 bar) 0.54 mol L⁻¹ (ZIF-8 20 wt%/Glycol 20 wt% + water 80 wt%, CH₄, 13.1 bar) 1.26 mol L⁻¹ (ZIF-8 20 wt%/Glycol 20 wt% + water 80 wt%, C₂H₄, 8.1 bar) (Testing conditions: 293.15 K)	
ZIF-67	[C₆BIm₂][NTf₂]₂	7.853	1308.6	0.9595	1896.7 (porogen 10 wt%, 298 K)	Homogeneous	Stable	9.542 mmol g⁻¹	105
								(Testing conditions: porogen 10 wt%, CO₂, 298 K, 1 bar)	

Table 3 (continued)

Composition		Pore size (Å)	Specific surface area (m^2 g^{-1})	Pore volume (cm^3 g^{-1})	Viscosity (mP s)	Dispersity	Stability	Sorption capacity	Ref.
Porogen	Solvent								
ZIF-8 HKUST-1	$[P_{6,6,6,14}][NTf_2]$ $[P_{6,6,6,14}][Cl]$	—	—	—	—	Homogeneous	Stable	0.3482 mmol g^{-1} (CO_2) 0.1327 mmol g^{-1} (CH_4) (Testing conditions: ZIF-8/$[P_{6,6,6,14}][NTf_2]$, porogen 5 wt%, 303.14 K, 5 bar) 0.3839 CO_2 (testing conditions: ZIF-8/$[P_{6,6,6,14}][Cl]$, porogen 5 wt%, 303.14 K, 5 bar) 0.3168 (testing conditions: HKUST-1/$[P_{6,6,6,14}][NTf_2]$, porogen 5 wt%, 303.14 K, 5 bar)	106
ZIF-67	Glycol–2-methylimidazole	—	—	—	74.7 (293.2 K)	Slurry	—	1.3 mol L^{-1} (testing conditions: ZIF-8 15 wt%/MIM 34 wt% + glycol 51 wt%, 303.2 K, 1 bar)	107
ZIF-8	Glycol–water	—	—	—	19.03	Slurry	—	0.68 mol L^{-1} (testing conditions: ZIF-8 20.2 wt%/Water 63.84 wt% + glycol 15.96 wt%, 293.15 K, CO_2, 2.9 bar)	108
ZIF-7 ZIF-8 ZIF-62	1-Methylimidazole Triethylene glycol Di(propylene glycol) butyl ether 1,3,5-Triisopropylbenzene	5 to 18	500 1400 190	—	3.78(ZIF-8/MIM, porogen 10 wt%) 6.29(ZIF-62/TPB, porogen 10 wt%)	Homogeneous	Highly stable	4.2 mmol g^{-1} (ZIF-8/MIM) 1.3 mmol g^{-1} (ZIF-62/TPB) (Testing conditions: porogen 10 wt%, CO_2, 298 K, 10 bar)	109
H-ZSM-5	$[P_{66614}][Br]$ $[Aliquant_{336}][Cl]$ $[P_{4442}][Suc]$	5.4–5.6	362.7	0.304	9550 (298 K) 810 (363 K)	Homogeneous	Stable	2.83 wt% (H-ZSM-5/$[P66614][Br]$) 3.31 wt% (H-ZSM-5/$[Aliquant336][Cl]$) 1.75 wt% (H-ZSM-5/$[P4442][Suc]$) (Testing conditions: CO_2, 298 K, 10 bar)	110
ZIF-8	$[P_{6,6,6,14}][NTf_2]$ $[P_{4,4,4,4}][OAc]$ $[P_{4,4,4,4}][Lev]$	—	—	—	—	Homogeneous	Stable	0.0995 mmol g^{-1} (4.9614 w/w% ZIF-8/$[P6,6,6,14][NTf_2]$) 0.0210 mmol g^{-1} (4.9614 w/w% ZIF-8/0.75 wt% $[P6,6,6,14][NTf_2]$ + 0.25 wt% $[P4,4,4,4][OAc]$) 0.0642 mmol g^{-1} (4.9614 w/w% ZIF-8/0.5 wt% $[P6,6,6,14][NTf_2]$ + 0.5 wt% $[P4,4,4,4][OAc]$) 0.0168 mmol g^{-1} (4.9614 w/w% ZIF-8/0.25 wt% $[P6,6,6,14][NTf_2]$ + 0.75 wt% $[P4,4,4,4][OAc]$) 0.1373 mmol g^{-1} (ZIF-8/$[P4,4,4,4][Lev]$ 4.9614 w/w%) (Testing conditions: CO_2, 303 K, 5 bar)	111
UiO-66 UiO-66-NH$_2$	Poly(dimethyl siloxane) (PDMS4k)	—	—	—	6.85 (UiO-66(484)@xPDMS/PDMS4k, porogen 33.3 wt%) 7.57 (UiO-66(185)@xPDMS/PDMS4k, porogen 33.3 wt%)	Homogeneous	Stable	1.375 mmol g^{-1} (UiO-66(185)@xPDMS/PDMS4k, porogen 50 wt%) 1.295 mmol g^{-1} (UiO-66-NH$_2$/xPDMS/PDMS4k, porogen 50 wt%)	112

Table 3 (*continued*)

Composition		Pore size (Å)	Specific surface area (m² g⁻¹)	Pore volume (cm³ g⁻¹)	Viscosity (mP s)	Dispersity	Stability	Sorption capacity	Ref.
Porogen	Solvent								
UiO-66-Br₂					20.84 (UiO-66(185)@xPDMS/PDMS4k, porogen 50 wt%) (~293 K)			0.554 mmol g⁻¹ (UiO-66-Br₂@xPDMS/PDMS4k, porogen 50 wt%)	
MIL-101(Cr)								(Testing conditions: CO₂, 273 K, 1 bar)	
All modified with PDMS									
ZIF-8 modified with branched polyethyleneimine (BPEI)	Branched polyethyleneimine (BPEI)	8.52	1903.7	0.716	1700 (298 K)	Homogeneous	Stable	0.259 mmol g⁻¹ (ZIF-8-g-BPEI/BPEI, porogen 30 wt%)	113
								(Testing conditions: porogen 10 30 wt%, CO₂, 298 K, 10 bar)	
Hollow carbon nanospheres	Polymerized ionic liquids	—	—	—	Viscous	Homogeneous	Stable	4.66 wt%	114
								(Testing conditions: porogen 16.6 wt%, CO₂, 298 K, 10 bar)	
COF-300	3-(3-(4-Formylphenoxy propyl)-1-methyl-1*H*-imidazol-3-ium BArF)	5 to 14	—	—	Viscous	Homogeneous	Highly stable	More than 10 and 20-fold increase in CO₂ and CH₄ sorption than solvent, respectively (Testing conditions: porogen 20 wt%, 273 K, 0.03 P/P₀)	115
ZIF-8	Glycol-2-methylimidazole–water	—	—	—	Low viscosity	—	Low	1.47 mol L⁻¹ (testing conditions: ZIF-8 10 wt%/MIM 25 wt%+ water 40 wt% + glycol 35 wt%, CO₂, 303.15 K, 1 bar)	116
ZIF-8	[Bpy][NTf₂]	—	1228	—	—	Homogeneous	Stable	—	117
ZIF-8	[Epy][NTf₂] [Bpy][NTf₂] [Hpy][NTf₂] [Emim][NTf₂] [Bmim][NTf₂] [Hmim][NTf₂]	—	1228	—	—	Homogeneous	Stable	—	118

a homogeneous and stable PL. The *in situ* coupling strategy can produce PLs using varied structures such as porous carbon nitride, porous boron nitride, and polymers with intrinsic microporosity.[114] Recently, a novel type III PL based on COF was made. The outer shell of COF was functionalized to improve the dispersion stability of COF suspension in acetonitrile. Later, the COF suspension was mixed with BArF ionic liquid, with minimal aggregation in the ionic liquid. The resulting PL based on dispersing COF in the solvent was formed.[115]

Practical applications of porous iquids

PLs offer the ability to combine the process advantages of liquids with the favourable capacities of porous solids. The field of PLs is in its infancy. However, it is clear that to ensure that these materials reach their way into the application, a good understanding of their properties is reached. To date, the potential applications are only a fraction of what is possible

in terms of their potential. A core set of properties of these materials is their simultaneous porosity, fluidity, and tunability that can be customised quickly for facile implementation at an industrial scale in existing plants.[7]

The solubility of a particular target gas in PLs is not constant at a specific temperature and pressure. Instead, the solubility will be dictated by relative polarities, and functional groups. Besides, PLs can possess remarkably high solubility and also shape- and size selectivity. PLs can selectively dissolve one species with an extremely high amount due to shape and size fitting with cavities and no required work to create cavities and enable only it to undergo a reaction. This can cause lower required pressures and even smaller vessels with the potential for lower cost and reduced hazards.[6,30] In general terms, PLs can be used in any area that uses liquids.[78]

Adsorption is a distinct potential area of PLs application where they act as an adsorbent for selective separation (Fig. 8). Not only do PLs possess higher absorption capacity and efficiency compared to the solvent and can be engineered into continuous cyclic separation processes,[5,26,27] but also PLs can
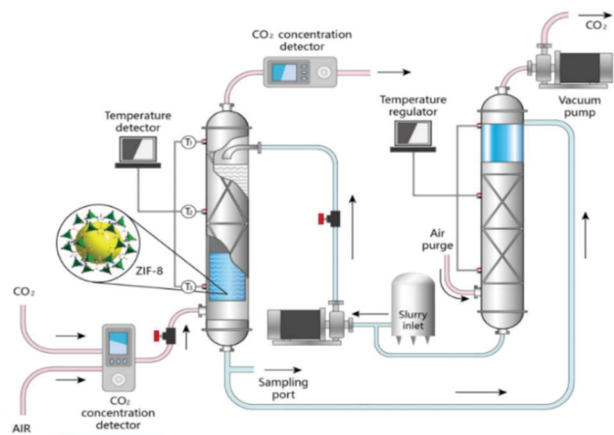
Fig. 8 Schematic diagram of the sorption-desorption unit using PLs (reproduced with permission,[116] Copyright 2020, American Chemical Society).

translate process from absorption to adsorption. Translation from absorption to adsorption means the high required regeneration energy significantly and adsorption enthalpy aspect compared to solvents decreases.[9] For instance, CO_2 capture by amine solutions is a traditional industrial process for CO_2 removal, and it is possible to upgrade the system to use PLs instead of amine solutions.[51,119]

Zhang *et al.* performed a fundamental molecular dynamics (MD) simulations study on the thermodynamics and kinetics of gas storage in PLs.[97] They simulated a PL consisting of dissolved functionalised porous cages with crown-ether in a 15-crown-5 solvent using molecular simulations.[3] They provide an insight into how to design PLs for targeting gas separation. It was observed that the gas storage capacity follows the order $CH_4 > CO_2 > N_2$, and so it is not a function of the gas molecule size. All the gases can enter the cavities without significant energy barriers and release quickly with only a low energy penalty. However, they favour different interactions with the porogen. For instance, CO_2 molecules favour the cavities while CH_4 molecules favour the cavities and the branches, and N_2 molecules are limited due to weak interactions with the cage. Thus, it was concluded that two factors govern the gas storage capacity, and the competition between them can determine the capacity. The first variable is non-electrostatic (dispersive) intermolecular interactions between the gas and the cage, which controls affinity. The second variable is the size and shape of the gas molecule, which controls whether the cavities are filled optimally.[97] Yin *et al.* also continued their study on this type of PLs using molecular dynamics simulations. The adsorption behaviour under pressure-swing adsorption (PSA) and temperature-swing adsorption (TSA) processes were evaluated. For this purpose, the working and separation capacities of CO_2/N_2 and CO_2/CH_4 systems were investigated. In the PSA process, the pressure range was 60 to 20 Bar at 298.15 K, and in the TSA process, the temperature was in the range of 400 to 298.15 K at 60 Bar. In both cases, PLs' working capacity can be decreased with increasing concentrations of cage molecules, while the separation can be enhanced.[98]

Chen *et al.* used dispersed ZIF-8 nanoparticles in glycol-water as type III PL to separate ethane from natural gas. They tried to perform experiments systematically, and they developed a thermodynamic model based on the results.[120] Recently, Li *et al.* used dispersed ZIF-8 nanoparticles in 2-methylimidazole, glycol, and water as PL type III for CO_2 separation for the first time in a pilot-scale packed tower. Based on experiments, the CO_2 cyclic capacity in the regeneration of CO_2-rich ZIF-8 slurry using pressure-swing adsorption was 0.26 mol L^{-1} under 0.1 MPa, eight times higher than that of the water washing method. Moreover, temperature-swing adsorption leads to a much higher CO_2 cyclic capacity (0.75 mol L^{-1} under 0.1 MPa) than that of ethanolamine solution, which means CO_2-rich ZIF-8 slurry needs less energy. Aspen Plus simulation distinguished the equivalent work of PL under the same condition is still lower compared to MEA solution, which means the process requires less work.[116]

Lai *et al.* formulated and evaluated PLs for the separation of ethane and ethene. The regeneration of porogens from solvents to study potential application in cyclic separation processes was investigated. They have found out that HKUST-1 in sesame oil has high adsorption but low selectivity. However, zeolite AgA in AgIL (Ag-containing ionic liquid) which possesses low chemical stability and regenerate ability, is very selective to ethane. Likewise, ethane-selective $Cu(Qc)_2$ (Qc = quinoline-5-carboxylate) in sesame oil and ZIF-7 in sesame oil are easily regenerated and have high chemical stabilities. Although ZIF-7 in sesame oil exhibits an interesting gated behaviour, $Cu(Qc)2$ in sesame oil displays the wider pressure range of ethane selectivity, easy synthesis procedure, and high stability leading to an interesting PL for ethane–ethene separation.[27] Yin *et al.* used density functional theory to systematically study the behaviour of CO_2 and sulphur dioxide (SO_2) absorptions using porous organic cages in hexachloropropene PL and silica-based porous ionic liquid, respectively. There are strong interactions between the PLs with CO_2 or SO_2. It is also possible to increase the gas absorption using different methods such as polymerization degree increments. These studies reveal the possibility of CO_2 and SO_2 capture to prevent the release of these acid gases into the environment.[121,122]

Catalysis by PLs may fill the gap between homogeneous and heterogeneous catalysis. Homogeneous and heterogeneous catalysts are limited by the availability of surface area on the catalyst after catalyst saturation with reactant molecules, and irrecoverability after the reaction completion, respectively.[124] Porous catalysts can indicate a larger number of catalytic sites per unit area and higher surface-to-volume ratios leading to a very high degree of interaction between catalyst and reactant molecules. On the other hand, the degree of interaction between catalyst and reactant molecules also depends on the catalyst phase which is higher in the liquid phase. Catalysis by PLs possesses both advantages and can achieve high selectivities for many industrial separations.[125,126] Recently, porous solids have been used to protect catalysts in PL catalysis, as represented in Fig. 9. Catalysts encapsulation does not change the catalyst's properties but also enhances it by preventing its
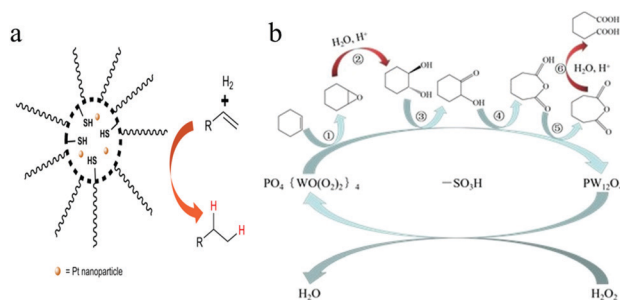
Fig. 9 Schematic diagram of PL catalysis (a) neat Pt@HS-SiO$_2$ PL (reproduced with permission,[85] Copyright 2020 Wiley-VCH); and (b) porous ionic liquid phosphotungstate (reproduced,[123] Open access).

aggregation. The easy aggregation of nanoparticles results in reduced catalytic effectiveness due to their high surface energies. These new developments provide a new path for future applications of PLs.[127]

Lately, Hemming *et al.* studied the catalytic capability of platinum nanoparticles encapsulated within hollow silica nanospheres liquefied with the corona-canopy method as a type I PL for hydrogenations of alkenes and nitroarenes.[68,85] It is also possible to dilute PL in alcohol, for instance, ethanol, to provide a faster reaction rate than a neat PL due to the system's high viscosity. Possibly these systems can find more applications in cascade reactions and especially systems with mutually incompatible catalysts.[85] Moreover, Bhattacharjee *et al.* have synthesised a new PL that can catalyse in-situ the conversion of adsorbed gases into the product. For this purpose, a composite PL based on polymer-surfactant modified hollow silica nanorods and carbonic anhydrase enzyme was prepared. This system's main advantage can be circulated catalytic PL easily in existing industrial plants and utilizing it for the post-

combustion chemisorption of CO$_2$. This class of PL stores CO$_2$ and then drive an *in situ* enzymatic hydration reaction of CO$_2$ to HCO$_3^-$ ion and eventually converting it to CaCO$_3$. This PL is not only able to absorb CO$_2$ but also can catalytically convert the adsorbed CO$_2$ to a non-hazardous product and hence offers a new route towards sustainable development.[82] Zhang *et al.* prepared a PL based on soluble and porous bistren cryptand covalent organic cages dissolved in methanol. The ultrafine Palladium nanoparticles were stabilized in the PL. The encapsulated PL was transferred onto g-carbon nitride nanosheets to serve as a co-catalyst. This combination provided an efficient heterogeneous photocatalytic hydrogen evolution from the water with long-term durability.[126] Recently, Wang *et al.* synthesized a porous ionic liquid as a heterogeneous catalyst by encapsulating 1-(3-sulfopropyl)morpholine phosphotungstate into MIL-101. It was used with H$_2$O$_2$ for the catalytic synthesis of adipic acid from cyclohexene. The experimental results of catalytic performance revealed that desired products had been successfully prepared. Moreover, the recycled catalytic performance of the catalyst under repeat 6 times proved the catalytically active substance was stable in the catalyst.[123] More recently Zou *et al.* have synthesised a MOF-based type I PL as a CO$_2$ stored reagent for catalysis. They have liquefied an imidazolium-functionalized UiO-66 with the corona-canopy method. This PL was able to adsorb a high concentration of CO$_2$. The adsorbed CO$_2$ could be released slowly from PL and efficiently utilized to synthesize cyclic carbonates in the atmosphere.[80]

As shown in Fig. 10, membranes based on PLs can be considered as another application. Liquid membranes based on PLs can cause high permeation and excellent selectivities, and at the same time, they also can be scaled up easily (Fig. 10a). Liquid membranes based on PLs take the advantages
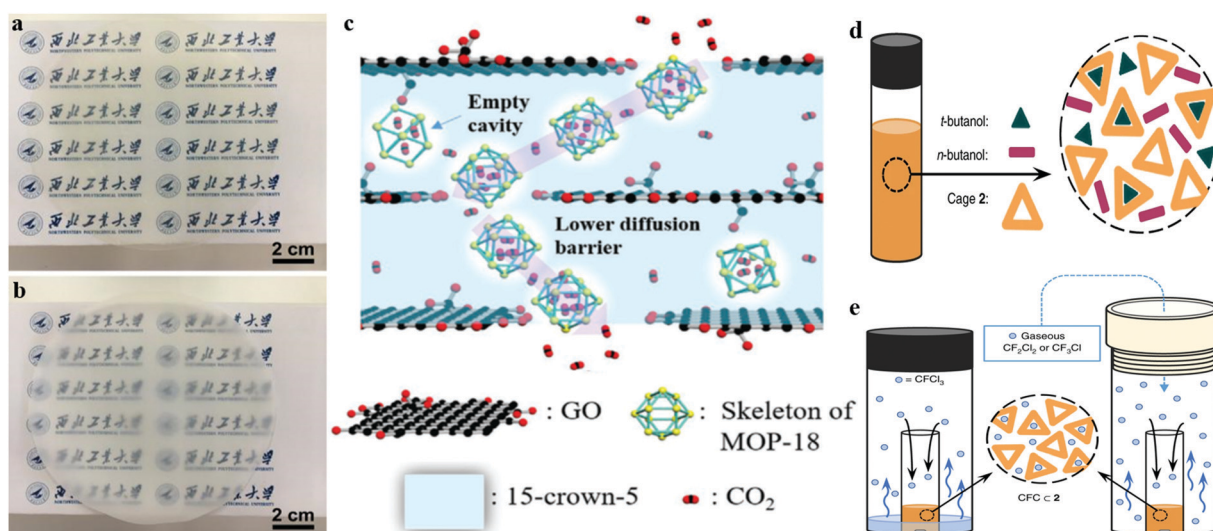

Fig. 10 The images of (a) 30 wt% UiO-66-OH based PL in Pebax; (b) 1 wt% UiO-66-OH in Pebax (reproduced with permission,[71] Copyright 2020 Elsevier); (c) the schematic diagram of the supported PL membrane (reproduced with permission,[102] Copyright 2020 Wiley-VCH); (d) shape selectivity of PLs in the encapsulation of isomers of several alcohols; and (e) capture chlorofluorocarbons in the cage as a PL (reproduced with permission,[65] Copyright 2020 Springer Nature).

of distillation, membrane, and adsorption simultaneously. Based on new research, these membranes provide fully tunable permeability to increase selectivity and create a bright future for these systems.[128] Deng *et al.* used dissolved with 5 wt% MOP-18 into 15-crown-5 as type II PL in a graphene oxide supported PL membrane. This class of membranes has higher permeance of gases such as H_2, CO_2, and N_2 than a graphene oxide supported 15-crown-5 membrane by 3.0, 4.0, and 2.7 times, respectively. The improved permeance can be attributed to the empty cavity of MOP-18 cages, which reducing the gas diffusion barrier.[102]

Mixed matrix membranes can be prepared from the high content of PL as filler and maintain the membranes' physical integrity due to their liquid nature, resulting in good compatibility between fillers and polymer matrixes (Fig. 10b).[9] Wang *et al.* incorporated PL into Pebax-1657 polymer matrix to form mixed matrix membranes (MMMs). They produced a PL using UiO-66-OH and the corona-canopy method. The UiO-66 PL, with an excellent homogeneous dispersion in the polymer matrix up to 30 wt%, lead to higher gas permeability.[71] 'Knebel *et al.* produced a very stable PL, resulting in PL co-processed with polymers and forming highly loaded MMMs. The external surface of ZIF-67 was modified using 1,3-bis (2,4,6-diisopropylphenyl)imidazole-2-ylidene (IDip) as a N-heterocyclic carbene. Then it was dispersed in a solvent to form PLs. PLs were blended with the 6FDA-DAM and 6FDA-DHTM-Durene polymers with over 40 wt% loading. The polymer swelling of MMMs was significantly reduced due to excellent filler–polymer intimate mixing, leading to excellent mechanical properties with an outstanding separation performance of propylene from propane.[129]

Membrane contactors are another configuration of the phase-contacting device, increasing the contact area for gas transfer and liquid–liquid extraction processes (Fig. 10d and e). Recently, some biocompatible post-synthetic MOFs for drug delivery have been used, even in PL. Desorption efficiency improvement of membrane contactors leads to their process's economic feasibility. PLs with negligible vapour pressure reduce the required energy consumption for recycling.[19] Ma *et al.* incorporated poly-(ethylene glycol)-imidazolium chains into a Zn-based ionic-liquid, porous, tetrahedral coordination cage. The resulting PLs represent higher shape and size selectivity in the encapsulation of isomers of several alcohols based on a stronger binding interaction due to better shape and size fit with the pores with respect to their isomers. This class of PL can also capture chlorofluorocarbons in the cage.[65]

Cahir *et al.* dispersed CD-MOF-1 as a porogen in olive oil as a solvent. CD-MOF-1 is a biocompatible MOF that was simply mixed with olive oil as a bulky solvent to form a homogeneous dispersion. This dispersion was stable for at least one day. The presence of empty pores was confirmed by higher gas adsorption than pure solvent a MOF alone. This biocompatible PL may be considered an example of PL with potential biomedical applications such as drug delivery.[50] PLs can also lead to chiral recognition and separation materials, the development of new drug screening mechanisms, biological separation, biosensors,
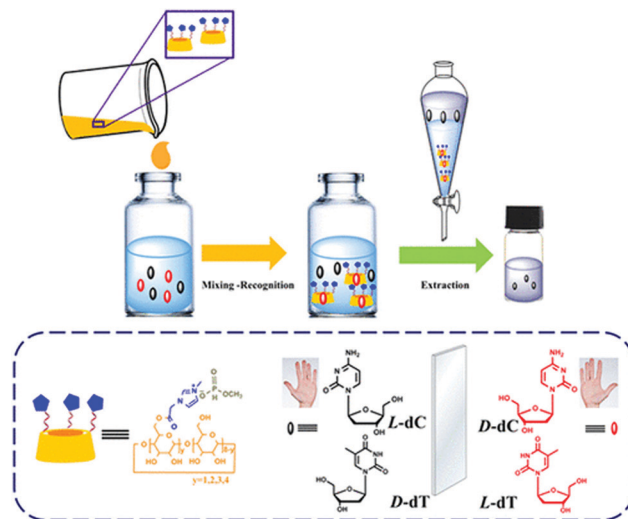

Fig. 11 Selective separation mechanism of nucleosides using γ-cyclodextrin PL (reproduced with permission,[130] Copyright 2020 American Chemical Society).

and biologically active medicines. Wang *et al.* developed a method to liquefy cyclodextrins by chemical modification (Fig. 11). The γ-cyclodextrin was esterified using imidazole-1-acetic chloride and forms omidazolyl-1-acetic cyclodextrin ester. Then, the reaction between the product and dimethyl phosphite lead to type I PL formation. The γ-cyclodextrin PL showed a remarkable chiral recognition ability toward pyrimidine nucleosides in water. The enantioselectivity of β-D-2-deoxycytidine from β-L-2-deoxythymidine reached 84.81%.[130] Moreover, based on a comparison between each vertex disordered PL with its associated scrambled cages, physical properties such as gas binding affinities are similar. However, some differences like the enantioselectivity of homochiral cages for chiral aromatic alcohols were not observed in corresponding homochiral PLs.[25]

During solvent extraction often referred to as liquid–liquid extraction, chemicals are separated based on their solubility in two immiscible liquids, typically polar and non-polar solvents. There is a huge demand to develop novel liquid absorbents to improve mass transfer performance and find green alternatives to traditional organic solvents used in extraction processes and ultimately bridge the gap between academic research and industrial challenges. PLs can combine classic characteristics of organic solvents with porous solids.[117,118] Wu *et al.* dispersed ZIF-8 in [Bpy][NTf₂] to investigate the extractive desulphurization of fuels. PL has shown extraction efficiencies of 72.41% Thiophene and 80.87% benzothiophene at 25 °C for 10 min. The remarkable sulphur compounds removal efficiencies are due to the synergistic effects of electrostatic interaction, hydrogen bonding, and π-complexation interaction among ZIF-8, [Bpy][NTf₂], and sulphur compounds. The reusability of PL also was confirmed by recycling tests (Fig. 12).[117] Wang *et al.* dispersed ZIF-8 in a broad range of ionic liquids including [Epy][NTf₂], [Bpy][NTf₂], [Hpy][NTf₂], [Emim][NTf₂], [Bmim][NTf₂], and[Hmim][NTf₂] to evaluate the extraction possibility of alcohol from aqueous solutions. ZIF-8/[Bpy][NTf₂] PL leads to a significant extraction
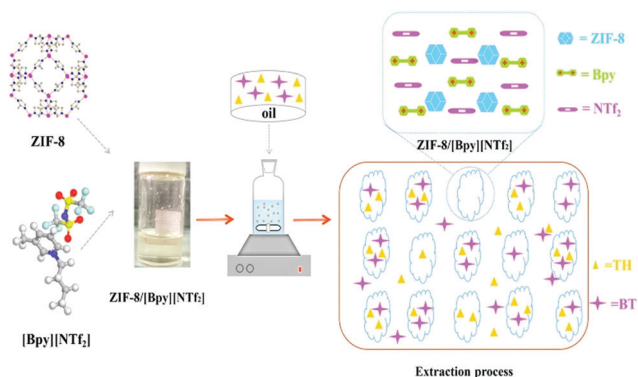
Fig. 12 Schematic diagram of solvent extraction using ZIF-8/[Bpy][NTf₂] PL (reproduced with permission,[117] Copyright 2021 Elsevier).

efficiency of 88.1% 2,2,3,3-tetrafluoro-1-propanol from its aqueous solution. The simple preparation procedure, easy recoverability, and proper reusability of PL are helpful in the optimization and design of effective PLs for similar applications.[118]

Challenges and opportunities

Limitations

Although there are high potential and opportunities for PLs, it still faces some limitations. Producing high free volume PLs with ideally zero volatility and fast guest adsorption and release kinetics to facilitate pressure-swing or temperature-swing adsorption/desorption cycles are the main limitations.[9] Furthermore, the PL production cost is high, and they need to be formulated economically. In general, type I PL often leads to low yield and complex production synthesis and conditions. These limit the industrial feasibility of type I PLs.

In contrast, type II and type III PLs are generally attractive due to their lower environmental risk and relatively cheaper starting materials. One of the main limitations is the selection of suitable sterically hindered solvents to prevent possible pore penetration. Possible agglomeration and sedimentation issues, and the necessity of any surface functionalization of porogens can be considered further limitations.[5,9]

When it comes to PLs, the traditional characterisation methods of porosity are unacceptable.[7] The presence of empty pores can be confirmed with higher gas adsorption compare to the pure solvent.[3] Even to perform adsorption, evaporation of the liquid at low pressures is another challenge. Density measurements also help to investigate the presence of free volume and, consequently, PL formation but these measurements are not highly accurate.[26] One useful, applicable technique is positron annihilation lifetime spectroscopy (PALS), which unfortunately is not widely available and requires complex data analysis.[7] Beside adding a small amount of a tiny competitor guest, the release of the dissolved gases can be considered as another method to confirm the presence of empty pores.[3]

Current and future developments of PL

This area is evolving quickly. Various remarkable applications in different fields confirm the potential applications of this new class of materials. The PLs combine the separation performances of solid materials in the liquid phase. This means PLs can easily be used in existing industrial plants without significant changes and budget to modify the industrial plants.[9]

Currently, much effort is devoted to finding appropriate combinations of solvents and porous solids, and much progress is being reported. In this regard, different types of PL have been synthesised and are still under further development. These other developments lead to a better understanding of PLs from both fundamental and applied perspectives. There are some interesting future development targets for PLs.[78] First, the development of applicable and available characterisation methods, or at least the computational screening method. Although there are some recognised and characterised materials already, there are some other materials that could also be PLs with further investigation.[31] Secondly, benchmarking PLs with high free-volume liquids is a good route to obtaining meaningful comparisons. A third development step can be directing synthesis towards zero volatility PLs, perhaps even a porous ionic liquid. Moreover, investigating adsorption and release kinetics of PLs should be another area of future investigations. There are some methods for the promotion of gas release from PLs such as ultrasonication; however, its scalability or cost-effectiveness is unclear.[25,78]

Outlook

Given the current interest among both academia and industry, the wide range of applications for PLs, and their diverse types and synthesis strategies,[2–4] it is predicted that the next few decades will be flooded with an immense amount of research related to PLs. Thus, researchers' imagination about PLs as a fast-growing research area can go beyond borders.[7]

Conclusions

The idea of PLs that combine the properties of fluidity and permanent porosity stimulate researchers' attention. The features of PLs, including porosity, low viscosity and stability lead to considerable properties such as very high gas solubility and fast gas diffusion. Thus, it attracts lots of attention from both the industry and the scientific world. This class of materials can be considered the next generation of liquids. They can be applied in any areas that use liquids, such as adsorption, catalysis, liquid membranes, and drug delivery.

Conflicts of interest

There are no conflicts to declare.

References

1 N. Giri, C. E. Davidson, G. Melaugh, M. G. Del Pópolo, J. T. A. Jones, T. Hasell, A. I. Cooper, P. N. Horton,

M. B. Hursthouse and S. L. James, *Chem. Sci.*, 2012, **3**, 2153–2157.

2 J. Zhang, S.-H. Chai, Z.-A. Qiao, S. M. Mahurin, J. Chen, Y. Fang, S. Wan, K. Nelson, P. Zhang and S. Dai, *Angew. Chem., Int. Ed.*, 2015, **54**, 932–936.

3 N. Giri, M. G. Del Pópolo, G. Melaugh, R. L. Greenaway, K. Rätzke, T. Koschine, L. Pison, M. F. C. Gomes, A. I. Cooper and S. L. James, *Nature*, 2015, **527**, 216–220.

4 G. Melaugh, N. Giri, C. E. Davidson, S. L. James and M. G. Del Pópolo, *Phys. Chem. Chem. Phys.*, 2014, **16**, 9422–9431.

5 S. L. James and B. Hutchings, *Functional Organic Liquids*, Wiley, 2019, 39–52.

6 S. L. James, *Adv. Mater.*, 2016, **28**, 5712–5716.

7 A. Bavykina, A. Cadiau and J. Gascon, *Coord. Chem. Rev.*, 2019, **386**, 85–95.

8 Y. Li, *ChemistrySelect*, 2020, **5**, 13664–13672.

9 M. Z. Ahmad and A. Fuoco, *Curr. Res. Green Sustainable Chem*, 2021, **4**, 100070.

10 P. F. Fulvio and S. Dai, *Chem*, 2020, **6**, 3263–3287.

11 K. Jie, Y. Zhou, H. P. Ryan, S. Dai and J. R. Nitschke, *Adv. Mater.*, 2021, **33**, e2005745.

12 I. D. Wilson, E. R. Adlard, M. Cooke and C. F. Poole, *Encyclopedia of Separation Science*, Academic Press, 2000.

13 M. Mohamedali, D. Nath, H. Ibrahim and A. Henni, *Greenhouse Gases*, 2016, 115–154.

14 D. L. Pavia, G. M. Lampman, G. S. Kriz and R. G. Engel, *Introduction to Organic Laboratory Techniques: A Small Scale Approach*, Cengage Learning, 2005.

15 J. D. Seader, E. J. Henley and D. K. Roper, *Separation Process Principles*, Wiley, 1998.

16 A. L. Yaumi, M. Z. A. Bakar and B. H. Hameed, *Energy*, 2017, **124**, 461–480.

17 N. Giri, M. G. Del Pópolo, G. Melaugh, R. L. Greenaway, K. Rätzke, T. Koschine, L. Pison, M. F. C. Gomes, A. I. Cooper and S. L. James, *Nature*, 2015, **527**, 216–220.

18 E. D. Bates, R. D. Mayton, I. Ntai and J. H. Davis, *J. Am. Chem. Soc.*, 2002, **124**, 926–927.

19 I. Abánades Lázaro, S. Haddad, S. Sacca, C. Orellana-Tavra, D. Fairen-Jimenez and R. S. Forgan, *Chem*, 2017, **2**, 561–578.

20 D. M. Cox, in *Nanostructure Science and Technology: R&D Status and Trends in Nanoparticles, Nanostructured Materials, and Nanodevices*, ed. R. W. Siegel, E. Hu, D. M. Cox, H. Goronkin, L. Jelinski, C. C. Koch, J. Mendel, M. C. Roco and D. T. Shaw, Springer Netherlands, Dordrecht, 1999, pp. 49–66.

21 M. Armand, F. Endres, D. R. MacFarlane, H. Ohno and B. Scrosati, *Nat. Mater.*, 2009, **8**, 621–629.

22 S. Sjostrom, H. Krutka, T. Starns and T. Campbell, *Energy Procedia*, 2011, **4**, 1584–1592.

23 V. Manovic and E. J. Anthony, *Int. J. Environ. Res. Public Health*, 2010, **7**, 3129–3140.

24 J. Fuchs, J. C. Schmid, S. Müller and H. Hofbauer, *Renewable Sustainable Energy Rev.*, 2019, **107**, 212–231.

25 R. L. Greenaway, D. Holden, E. G. B. Eden, A. Stephenson, C. W. Yong, M. J. Bennison, T. Hasell, M. E. Briggs, S. L. James and A. I. Cooper, *Chem. Sci.*, 2017, **8**, 2640–2651.

26 M. Costa Gomes, L. Pison, C. Červinka and A. Padua, *Angew. Chem., Int. Ed.*, 2018, **57**, 11909–11912.

27 B. Lai, J. Cahir, M. Y. Tsang, J. Jacquemin, D. Rooney, B. Murrer and S. L. James, *ACS Appl. Mater. Interfaces*, 2021, **13**, 932–936.

28 T. D. Bennett, F.-X. Coudert, S. L. James and A. I. Cooper, *Nat. Mater.*, 2021, **20**, 1179–1187.

29 A. Pohorille and L. R. Pratt, *J. Am. Chem. Soc.*, 1990, **112**, 5066–5074.

30 R. A. Pierotti, *Chem. Rev.*, 1976, **76**, 717–726.

31 N. O'Reilly, N. Giri and S. L. James, *Chem. – Eur. J.*, 2007, **13**, 3020–3025.

32 A. Zinke and E. Ziegler, *Chem. – Eur. J.*, 1944, **77**, 264–272.

33 C. J. Pedersen, *Angew. Chem., Int. Ed. Engl.*, 1988, **27**, 1021–1027.

34 J. D. van Loon, W. Verboom and D. N. Reinhoudt, *Org. Prep. Proced. Int.*, 1992, **24**, 437–462.

35 A. Flinn, G. C. Hough, J. F. Stoddart and D. J. Williams, *Angew. Chem., Int. Ed. Engl.*, 1992, **31**, 1475–1477.

36 T. A. Robbins, C. B. Knobler, D. R. Bellew and D. J. Cram, *J. Am. Chem. Soc.*, 1994, **116**, 111–122.

37 J. L. Atwood and J. M. Lehn, *Comprehensive Supramolecular Chemistry: Supramolecular Technology*, Pergamon, 1996.

38 M. R. Caira, S. A. Bourne, W. T. Mhlongo and P. M. Dean, *Chem. Commun.*, 2004, 2216–2217.

39 J. Lerchner, R. Kirchner, J. Seidel, D. Wählisch, G. Wolf, W. A. König and R. Lucklum, *Thermochim. Acta*, 2006, **445**, 98–103.

40 S. C. Hsu, M. Ramesh, J. H. Espenson and T. B. Rauchfuss, *Angew. Chem., Int. Ed.*, 2003, **42**, 2663–2666.

41 M. Yamada, M. Arai, M. Kurihara, M. Sakamoto and M. Miyake, *J. Am. Chem. Soc.*, 2004, **126**, 9482–9483.

42 A. B. Bourlinos, R. Herrera, N. Chalkias, D. D. Jiang, Q. Zhang, L. A. Archer and E. P. Giannelis, *Adv. Mater.*, 2005, **17**, 234–237.

43 A. B. Bourlinos, S. Ray Chowdhury, R. Herrera, D. D. Jiang, Q. Zhang, L. A. Archer and E. P. Giannelis, *Adv. Funct. Mater.*, 2005, **15**, 1285–1290.

44 S. C. Warren, M. J. Banholzer, L. S. Slaughter, E. P. Giannelis, F. J. DiSalvo and U. B. Wiesner, *J. Am. Chem. Soc.*, 2006, **128**, 12074–12075.

45 A. Devaux, Z. Popović, O. Bossart, L. De Cola, A. Kunzmann and G. Calzaferri, *Microporous Mesoporous Mater.*, 2006, **90**, 69–72.

46 K. E. Chaffee, H. A. Fogarty, T. Brotin, B. M. Goodson and J.-P. Dutasta, *J. Phys. Chem. A*, 2009, **113**, 13675–13684.

47 N. Hosono, M. Gochomori, R. Matsuda, H. Sato and S. Kitagawa, *J. Am. Chem. Soc.*, 2016, **138**, 6525–6531.

48 W. Shan, P. F. Fulvio, L. Kong, J. A. Schott, C.-L. Do-Thanh, T. Tian, X. Hu, S. M. Mahurin, H. Xing and S. Dai, *ACS Appl. Mater. Interfaces*, 2018, **10**, 32–36.

49 B. Hosseini Monjezi, K. Kutonova, M. Tsotsalas, S. Henke and A. Knebel, *Angew. Chem., Int. Ed.*, 2021, **60**, 15153–15164.

50 J. Cahir, M. Y. Tsang, B. Lai, D. Hughes, M. A. Alam, J. Jacquemin, D. Rooney and S. L. James, *Chem. Sci.*, 2020, **11**, 2077–2084.

51 H. Liu, B. Liu, L.-C. Lin, G. Chen, Y. Wu, J. Wang, X. Gao, Y. Lv, Y. Pan, X. Zhang, X. Zhang, L. Yang, C. Sun, B. Smit and W. Wang, *Nat. Commun.*, 2014, **5**, 5147.

52 X. Zhao, Y. Yuan, P. Li, Z. Song, C. Ma, D. Pan, S. Wu, T. Ding, Z. Guo and N. Wang, *Chem. Commun.*, 2019, **55**, 13179–13182.

53 A. Vashchuk, A. Fainleib, O. Starostenko and D. Grande, *Express Polym. Lett.*, 2018, **12**, 898–917.

54 J. Dupont, *Acc. Chem. Res.*, 2011, **44**, 1223–1231.

55 P. Wasserscheid and T. Welton, *Ionic Liquids in Synthesis*, Wiley, 2008.

56 A. Knorr and R. Ludwig, *Sci. Rep.*, 2015, **5**, 1–7.

57 J. Sun, M. Forsyth and D. R. Macfarlane, *J. Phys. Chem. B*, 1998, **102**, 8858–8864.

58 E. I. Izgorodina, M. Forsyth and D. R. MacFarlane, *Aust. J. Chem.*, 2007, **60**, 15–20.

59 J. Golding, S. Forsyth, D. R. MacFarlane, M. Forsyth and G. B. Deacon, *Green Chem.*, 2002, **4**, 223–229.

60 E. I. Izgorodina, U. L. Bernard, P. M. Dean, J. M. Pringle and D. R. MacFarlane, *Cryst. Growth Des.*, 2009, **9**, 4834–4839.

61 S. Zhang, K. Dokko and M. Watanabe, *Chem. Sci.*, 2015, **6**, 3684–3691.

62 A. Shinohara, C. Pan, L. Wang and T. Nakanishi, *Mol. Syst. Des. Eng.*, 2019, **4**, 78–90.

63 N. J. Fernandes, T. J. Wallin, R. A. Vaia, H. Koerner and E. P. Giannelis, *Chem. Mater.*, 2014, **26**, 84–96.

64 S. Liu, J. Liu, X. Hou, T. Xu, J. Tong, J. Zhang, B. Ye and B. Liu, *Langmuir*, 2018, **34**, 3654–3660.

65 L. Ma, C. J. E. Haynes, A. B. Grommet, A. Walczak, C. C. Parkins, C. M. Doherty, L. Longley, A. Tron, A. R. Stefankiewicz, T. D. Bennett and J. R. Nitschke, *Nat. Chem.*, 2020, **12**, 270–275.

66 K. Jie, N. Onishi, J. A. Schott, I. Popovs, D.-E. Jiang, S. Mahurin and S. Dai, *Angew. Chem., Int. Ed.*, 2020, **59**, 2268–2272.

67 P. Li, J. A. Schott, J. Zhang, S. M. Mahurin, Y. Sheng, Z.-A. Qiao, X. Hu, G. Cui, D. Yao, S. Brown, Y. Zheng and S. Dai, *Angew. Chem., Int. Ed.*, 2017, **56**, 14958–14962.

68 E. B. Hemming, A. F. Masters and T. Maschmeyer, *Chem. Commun.*, 2019, **55**, 11179–11182.

69 X. Zhao, S. An, J. Dai, C. Peng, J. Hu and H. Liu, *New J. Chem.*, 2020, **44**, 12715–12722.

70 T. Shi, Y. Zheng, T. Wang, P. Li, Y. Wang and D. Yao, *ChemPhysChem*, 2018, **19**, 130–137.

71 D. Wang, Y. Xin, X. Li, F. Wang, Y. Wang, W. Zhang, Y. Zheng, D. Yao, Z. Yang and X. Lei, *Chem. Eng. J.*, 2020, **416**, 127625.

72 F. Su, X. Li, Y. Wang, Z. He, L. Fan, H. Wang, J. Xie, Y. Zheng and D. Yao, *Sep. Purif. Technol.*, 2021, **277**, 119410.

73 L. Sheng, Z. Chen and Y. Wang, *Appl. Surf. Sci.*, 2021, **536**, 147951.

74 L. Sheng and Z. Chen, *J. Mol. Liq.*, 2021, **333**, 115890.

75 L. Sheng, Z. Chen, B. Xu and J. Shi, *J. Phys. Chem. B*, 2021, **125**, 5387–5396.

76 J. Ben Ghozi-Bouvrande, S. Pellet-Rostaing and S. Dourdain, *Nanomaterials*, 2021, **11**, 2307.

77 M. Mastalerz, *Nature*, 2015, **527**, 174–176.

78 A. I. Cooper, *ACS Cent. Sci.*, 2017, **3**, 544–553.

79 Y. Liu, Y. Bai and T. Tian, *Materials*, 2019, **12**, 3984.

80 Y. H. Zou, Y. B. Huang, D. H. Si, Q. Yin, Q. J. Wu, Z. Weng and R. Cao, *Angew. Chem., Int. Ed.*, 2021, **60**, 20915–20920.

81 R. Kumar, P. Dhasaiyan, P. M. Naveenkumar and K. P. Sharma, *Nanoscale Adv.*, 2019, **1**, 4067–4075.

82 A. Bhattacharjee, R. Kumar and K. P. Sharma, *ChemSusChem*, 2021, **14**, 3303–3314.

83 D. Wang, Y. Xin, X. Li, H. Ning, Y. Wang, D. Yao, Y. Zheng, Z. Meng, Z. Yang, Y. Pan, P. Li, H. Wang, Z. He and W. Fan, *ACS Appl. Mater. Interfaces*, 2021, **13**, 2600–2609.

84 X. Li, D. Yao, D. Wang, Z. He, X. Tian, Y. Xin, F. Su, H. Wang, J. Zhang, X. Li, M. Li and Y. Zheng, *Chem. Eng. J.*, 2021, **429**, 132296.

85 E. B. Hemming, A. F. Masters and T. Maschmeyer, *Chem. – Eur. J.*, 2020, **73**, 1296–1300.

86 S. L. James, M. Y. Tsang, J. Cahir and D. Rooney, *U.S. Patent*, 2020, **No. 2020/0330919**, A1.

87 J. B. Nagy, *Synthesis, Characterization and Use of Zeolitic Microporous Materials*, DecaGen, 1998.

88 T. Hasell and A. I. Cooper, *Nat. Rev. Mater*, 2016, **1**, 16053.

89 D. J. Tranchemontagne, Z. Ni, M. O'Keeffe and O. M. Yaghi, *Angew. Chem., Int. Ed.*, 2008, **47**, 5136–5147.

90 J. D. Evans, C. J. Sumby and C. J. Doonan, *Chem. Lett.*, 2015, **44**, 582–588.

91 C. S. Diercks and O. M. Yaghi, *Science*, 2017, **355**, 6328.

92 J. C. Garcia, J. F. Justo, W. V. M. Machado and L. V. C. Assali, *Phys. Rev. B: Condens. Matter Mater. Phys.*, 2009, **80**, 125421.

93 A. P. Côté, A. I. Benin, N. W. Ockwig, M. Keeffe, A. J. Matzger and O. M. Yaghi, *Science*, 2005, **310**, 1166–1170.

94 A. B. Marco, D. Cortizo-Lacalle, I. Perez-Miqueo, G. Valenti, A. Boni, J. Plas, K. Strutyński, S. De Feyter, F. Paolucci, M. Montes, A. N. Khlobystov, M. Melle-Franco and A. Mateo-Alonso, *Angew. Chem., Int. Ed.*, 2017, **56**, 6946–6951.

95 T. Ben and S. Qiu, *CrystEngComm*, 2013, **15**, 17–26.

96 U. Vagt and C. Emmanuel, *Chem. Processing*, 2006, **69**, 45.

97 F. Zhang, F. Yang, J. Huang, B. G. Sumpter and R. Qiao, *J. Phys. Chem. B*, 2016, **120**, 7195–7200.

98 Z. Yin, H. Chen, L. Yang, C. Peng, Y. Qin, T. Wang, W. Sun and C. Wang, *Langmuir*, 2021, **37**, 1255–1266.

99 R. J. Kearsey, B. M. Alston, M. E. Briggs, R. L. Greenaway and A. I. Cooper, *Chem. Sci.*, 2019, **10**, 9454–9465.

100 B. D. Egleston, K. V. Luzyanin, M. C. Brand, R. Clowes, M. E. Briggs, R. L. Greenaway and A. I. Cooper, *Angew. Chem., Int. Ed.*, 2020, **19**, 7432–7436.

101 M. Atilhan, A. Cincotti and S. Aparicio, *J. Mol. Liq.*, 2021, **330**, 115660.

102 Z. Deng, W. Ying, K. Gong, Y.-J. Zeng, Y. Yan and X. Peng, *Small*, 2020, **16**, 1907016.

103 Z. Lei, C. Dai and W. Song, *Chem. Eng. Sci.*, 2015, **127**, 260–268.

104 H. Liu, Y. Pan, B. Liu, C. Sun, P. Guo, X. Gao, L. Yang, Q. Ma and G. Chen, *Sci. Rep.*, 2016, **6**, 1–11.

105 X. Li, D. Wang, Z. He, F. Su, N. Zhang, Y. Xin, H. Wang, X. Tian, Y. Zheng, D. Yao and M. Li, *Chem. Eng. J.*, 2021, **417**, 129239.

106 J. Avila, C. Červinka, P.-Y. Dugas, A. A. H. Pádua and M. Costa Gomes, *Adv. Mater. Interfaces*, 2021, **8**, 2001982.

107 Y. Pan, H. Li, X.-X. Zhang, Z. Zhang, X.-S. Tong, C.-Z. Jia, B. Liu, C.-Y. Sun, L.-Y. Yang and G.-J. Chen, *Chem. Eng. Sci.*, 2015, **137**, 504–514.

108 H. Li, X. Gao, C. Jia, W. Chen, B. Liu, L. Yang, C. Sun and G. Chen, *Energies*, 2018, **11**, 1890.

109 H. Mahdavi, H. Zhang, L. K. Macreadie, C. M. Doherty, D. Acharya, S. J. D. Smith, X. Mulet and M. R. Hill, *Nano Res.*, 2021, 1–6.

110 P. Li, H. Chen, J. A. Schott, B. Li, Y. Zheng, S. M. Mahurin, D.-E. Jiang, G. Cui, X. Hu and Y. Wang, *Nanoscale*, 2019, **11**, 1515–1519.

111 J. Avila, L. F. Lepre, C. Santini, M. Tiano, S. Denis-Quanquin, K. C. Szeto, A. Padua and M. C. Gomes, *Angew. Chem., Int. Ed.*, 2020, **60**, 12876–12882.

112 S. He, L. Chen, J. Cui, B. Yuan, H. Wang, F. Wang, Y. Yu, Y. Lee and T. Li, *J. Am. Chem. Soc.*, 2019, **141**, 19708–19714.

113 X. Li, D. Wang, H. Ning, Y. Xin, Z. He, F. Su, Y. Wang, J. Zhang, H. Wang, L. Qian, Y. Zheng, D. Yao and M. Li, *Sep. Purif. Technol.*, 2021, **276**, 119305.

114 P. Li, D. Wang, L. Zhang, C. Liu, F. Wu, Y. Wang, Z. Wang, Z. Zhao, W. Wu, Y. Liang, Z. Li, W. Wang and Y. Zheng, *Small*, 2021, **17**, 2006687.

115 R. E. Mow, A. S. Lipton, S. Shulda, E. A. Gaulding, T. Gennett and W. A. Braunecker, *J. Mater. Chem. A*, 2020, **8**, 23455–23462.

116 H. Li, B. Liu, M. Yang, D. Zhu, Z. Huang, W. Chen, L. Yang and G. Chen, *Ind. Eng. Chem. Res.*, 2020, **59**, 6154–6163.

117 J. Wu, X. Wu, P. Zhao, Z. Wang, L. Zhang, D. Xu and J. Gao, *Fuel*, 2021, **300**, 121013.

118 Z. Wang, P. Zhao, J. Wu, J. Gao, L. Zhang and D. Xu, *New J. Chem.*, 2021, **45**, 8557–8562.

119 J. Zhang, N. Lv, Y. Chao, L. Chen, W. Fu, J. Yin, H. Li, W. Zhu and H. Li, *J. Mol. Graphics Modell.*, 2020, 107694.

120 W. Chen, E. Zou, J. Y. Zuo, M. Chen, M. Yang, H. Li, C. Jia, B. Liu, C. Sun, C. Deng, Q. Ma, L. Yang and G. Chen, *Ind. Eng. Chem. Res.*, 2019, **58**, 9997–10006 6.

121 J. Yin, W. Fu, J. Zhang, H. Ran, N. Lv, Y. Chao, H. Li, W. Zhu, H. Liu and H. Li, *RSC Adv.*, 2020, **10**, 42706–42717.

122 J. Yin, J. Zhang, W. Fu, D. Jiang, N. Lv, H. Liu, H. Li and W. Zhu, *J. Mol. Graphics Modell.*, 2021, **103**, 107788.

123 H. Wang, L. Wang, X. Zeng and Y. Wang, *J. Inorg. Organomet. Polym. Mater.*, 2021, **31**, 1–14.

124 I. Bertini, *Inorganic and Bio-Inorganic Chemistry*, EOLSS Publications, 2009, vol. 2.

125 D. Wang, Y. Xin, D. Yao, X. Li, H. Ning, H. Zhang, Y. Wang, X. Ju, Z. He, Z. Yang, W. Fan, P. Li and Y. Zheng, *Adv. Funct. Mater.*, 2022, **32**, 2104162.

126 J. H. Zhang, M. J. Wei, Y. L. Lu, Z. W. Wei, H. P. Wang and M. Pan, *ACS Appl. Energy Mater.*, 2020, **3**, 12108–12114.

127 C. García-Simón, R. Gramage-Doria, S. Raoufmoghaddam, T. Parella, M. Costas, X. Ribas and J. N. H. Reek, *J. Am. Chem. Soc.*, 2015, **137**, 2680–2687.

128 H. Liu, Y. Pan, B. Liu, C. Sun, P. Guo, X. Gao, L. Yang, Q. Ma and G. Chen, *Sci. Rep.*, 2016, **6**, 1–11.

129 A. Knebel, A. Bavykina, S. J. Datta, L. Sundermann, L. Garzon-Tovar, Y. Lebedev, S. Durini, R. Ahmad, S. M. Kozlov, G. Shterk, M. Karunakaran, I. D. Carja, D. Simic, I. Weilert, M. Klüppel, U. Giese, L. Cavallo, M. Rueping, M. Eddaoudi, J. Caro and J. Gascon, *Nat. Mater.*, 2020, **19**, 1346–1353.

130 Y. Wang, Y. Sun, H. Bian, L. Zhu, D. Xia and H. Wang, *ACS Appl. Mater. Interfaces*, 2020, **12**, 45916–45928.